

T 1476

FACTORS AFFECTING SIGMA PHASE PRECIPITATION
IN AN AUSTENITIC STAINLESS STEEL
WELD DEPOSIT

ARTHUR LAKES LIBRARY
COLORADO SCHOOL OF MINES
GOLDEN, COLORADO

By

Alan L. Liby

ProQuest Number: 10781790

All rights reserved

INFORMATION TO ALL USERS

The quality of this reproduction is dependent upon the quality of the copy submitted.

In the unlikely event that the author did not send a complete manuscript and there are missing pages, these will be noted. Also, if material had to be removed, a note will indicate the deletion.



ProQuest 10781790

Published by ProQuest LLC (2018). Copyright of the Dissertation is held by the Author.

All rights reserved.

This work is protected against unauthorized copying under Title 17, United States Code
Microform Edition © ProQuest LLC.

ProQuest LLC.
789 East Eisenhower Parkway
P.O. Box 1346
Ann Arbor, MI 48106 – 1346

A Thesis submitted to the Faculty and the Board of Trustees of the Colorado School of Mines in partial fulfillment of the requirements for the degree of Master of Science.

Signed: Alan S. Liby

Golden, Colorado

Date: May 5, 1972

Approved: Donald T. Klodt
Donald T. Klodt
Thesis Advisor

John P. Hager
John P. Hager
Head, Department of
Metallurgical Engineering

ARTHUR LAKES LIBRARY
COLORADO SCHOOL OF MINES
GOLDEN, COLORADO

Golden, Colorado

Date: May 8, 1972

ABSTRACT

Factors affecting formation of the sigma phase were observed in specimens prepared by depositing ER 309 filler metal on type 304 stainless steel plate using the gas-metal arc-welding process.

As-welded and solution annealed specimens were aged at 1350^o F for up to 500 hr to promote the formation of sigma. Transformations resulting from the aging treatment were followed by systematic optical metallography using a variety of etchants. X-ray diffraction, electron-probe microanalysis, and hardness testing were also used in an attempt to follow the transformation.

Alloy element redistribution during weld solidification and subsequent heat treatment was found to be significant in transformation of the duplex austenite:ferrite stainless steel microstructures studied.

CONTENTS

Introduction.....	1
Background.....	2
Austenite.....	2
Occurrence.....	2
Structure and Properties.....	6
Ferrite.....	6
Occurrence.....	7
Properties.....	7
Carbides.....	9
Occurrence.....	9
Effects.....	10
The Sigma Phase.....	10
Physical Characteristics.....	11
Structure.....	11
Occurrence.....	12
The Sigma Phase in Commercial Alloys.....	12
Sigma in Ferritic Fe-Cr Alloys.....	13
Sigma in Austenitic Fe-Cr-Ni Alloys.....	15
Effect of Sigma Phase on the Properties of Alloys..	19
Experimental Procedures and Results	21
Selection of Alloys.....	21

Filler Metal.....	21
Base Metal.....	21
Welding.....	24
Heat Treatment.....	26
Solutionizing Treatment.....	26
Aging Treatment.....	26
Metallography.....	27
Preparation.....	27
Etching.....	27
Photomicrography.....	30
X-ray Diffraction.....	54
Hardness Measurements.....	58
Microprobe Analysis.....	59
Discussion.....	65
Weld Solidification Structure.....	65
Solidification Mode.....	65
Segregation.....	67
Nature of Observed Transformations.....	70
Transformation of the as-welded Structure.....	70
Transformation of the Solutionized Structure.....	71
Conclusions.....	74
Suggestions for Further Research.....	75
Literature Cited.....	77

FIGURES

1.	Constitution of Fe-Ni and Fe-Cr binary alloys.....	4
2.	Phase relationships in the Fe-Cr-Ni ternary system.....	5
3.	Constitution diagram for stainless steel weld metal.....	8
4.	Sigma phase in the Fe-Cr binary.....	14
5.	Effect of commercial impurities on sigma formation.....	14
6.	Location of commercial compositions in the Fe-Cr-Ni ternary system.....	17
7.	Estimation of weld deposit composition and structure using the Schaeffler diagram.....	23
8.	Photomicrograph of ER 309 filler metal on type 304 stainless steel base.....	25
9.	Specimen in as-welded condition. 720X.....	31
10.	Specimen in as-welded condition. 1500X.....	32
11.	As-welded specimen aged at 1350 ^o F for 1 hr. 1000X.....	33
12.	As-welded specimen aged at 1350 ^o F for 4 hr. 1000X.....	34
13.	As-welded specimen aged at 1350 ^o F for 24 hr. 1500X.....	35
14.	As-welded specimen aged at 1350 ^o F for 24 hr. 1500X.....	36
15.	As-welded specimen aged at 1350 ^o F for 24 hr. 720X.....	37

16.	As-welded specimen aged at 1350 ^o F for 24 hr. 1500X.....	38
17.	As-welded specimen aged at 1350 ^o F for 24 hr. 1500X.....	39
18.	As-welded specimen aged at 1350 ^o F for 24 hr. 500X.....	40
19.	As-welded specimen aged at 1350 ^o F for 100 hr. 1000X.....	41
20.	As-welded specimen aged at 1350 ^o F for 500 hr. 1000X.....	42
21.	As-welded specimen solutionized at 2000 ^o F followed by water quench. 720X.....	43
22.	As-welded specimen solutionized at 2000 ^o F followed by water quench. 1500X.....	44
23.	Solution annealed specimen aged at 1350 ^o F for 20 min. 1500X.....	45
24.	Solution annealed specimen aged at 1350 ^o F for 1 hr. 1500X.....	46
25.	Solution annealed specimen aged at 1350 ^o F for 4 hr. 1500X.....	47
26.	Solution annealed specimen aged at 1350 ^o F for 4 hr. 1500X.....	48
27.	Solution annealed specimen aged at 1350 ^o F for 24 hr. 1500X.....	49
28.	Solution annealed specimen aged at 1350 ^o F for 24 hr. 1500X.....	50
29.	Solution annealed specimen aged at 1350 ^o F for 24 hr. 1500X.....	51
30.	Solution annealed specimen aged at 1350 ^o F for 24 hr. 1000X.....	52
31.	Solution annealed specimen aged at 1350 ^o F for 24 hr. 500X.....	53
32.	Typical x-ray diffraction patterns obtained from cold-worked and annealed filings.....	56
33.	X-ray diffraction patterns obtained after dissolving matrix in Fe-Cl ₃ solution.....	57

34.	Microhardness traverse in specimen aged 1350° F for 1 hr. 0.1 Kg load. 250X.....	60
35.	Microhardness indentations at 1000X.....	61
36.	X-ray image of chromium distribution in as- deposited weld. 1000X.....	62

TABLES

1. Nominal composition of filler and base metals.....	22
2. Etching reagents employed.....	28

88 Hines

ACKNOWLEDGEMENTS

The author gratefully acknowledges the guidance and advice provided by Dr. D.T. Klodt throughout the course of this research.

Financial support for this investigation was provided by the Colorado School of Mines Foundation, Inc.

A special thanks is extended to Judie, Chris, and Pat, whose patience and understanding were limitless.

INTRODUCTION

The widespread commercial application of austenitic Cr-Ni stainless steels during the past forty years has resulted in the publishing of numerous studies of the physical metallurgy of these alloys. The welding metallurgy of these steels has also received considerable attention.

This study is directed toward the characterization of the microstructure of an austenitic stainless steel weld deposit. The primary effect to be considered is the effect of weld solidification and thermal history upon alloy composition and progression of precipitation of secondary phases in an austenitic matrix. The factors affecting the precipitation of one such secondary phase, sigma, will form the central theme for this investigation. The occurrence of sigma phase in austenitic stainless steels is of importance because of its deleterious effects upon mechanical and corrosion properties of these alloys.

Multi-component engineering alloy systems do not lend themselves easily to the study of fundamental metallurgical phenomena, yet there is a real need to attempt to explain and predict the behavior of these alloys based on the knowledge gained by study of simple systems. This study is such an attempt.

BACKGROUND

Alloys for this study were chosen so as to consist of as many as four phases, depending upon thermal history. The observed phases are austenite, ferrite, carbides, and sigma. The nature of these phases and their effect upon the properties of austenitic stainless steels will be discussed by way of review of the prior literature.

Austenite

Austenite, the face-centered cubic phase in iron-base alloys, forms the matrix for the alloys to be studied. The relationship of austenite to the other phases in Fe-Cr-Ni alloys will be discussed in terms of the binary and ternary phase diagrams presented in figures 1 and 2.¹

Occurrence. Although the equilibrium diagrams of figures 1 and 2 are of little use in predicting the structures of commercial alloys which have been rapidly cooled, they are of value in illustrating the effects of various alloying elements on the resulting structure of these alloys.

Figure 1(a) shows the binary equilibrium diagram between iron and nickel. Notice that increasing additions of nickel to pure iron expands the temperature range over which austenite, γ , is the equilibrium phase. Nickel is thus an

austenitizer or austenite stabilizing element. Other elements which are commonly encountered in commercial Cr-Ni stainless steels and which have the same effect as nickel are carbon, nitrogen, and manganese.

The effect of increasing additions of chromium on the observed equilibrium structure of iron-base alloys as a function of temperature is shown in figure 1(b). In this case the temperature range over which austenite is the stable phase is contracted with an increase in chromium content. The phase actually closes upon itself and, beyond a chromium content of 13 wt% the austenite phase is no longer observed. Chromium thus is a "deaustenitizer" or ferrite stabilizer. Other elements providing this same effect include silicon, molybdenum, and niobium.

The combined effect of chromium and nickel on the equilibrium structures at elevated temperatures is shown in figure 2(a), (b), (c). These diagrams give an indication of the structures encountered at room temperature because of the sluggishness of further transformation as the temperature goes lower. In the range of compositions of commercial Cr-Ni stainless steels (15-25% Cr, 7-15% Ni) the diagrams show the possible formation of three different phases; austenite, ferrite, and sigma. In commercial alloys the situation is complicated considerably by the presence of minor quantities of other elements. For example chromium carbides readily form at intermediate temperatures thereby reducing the ferrite

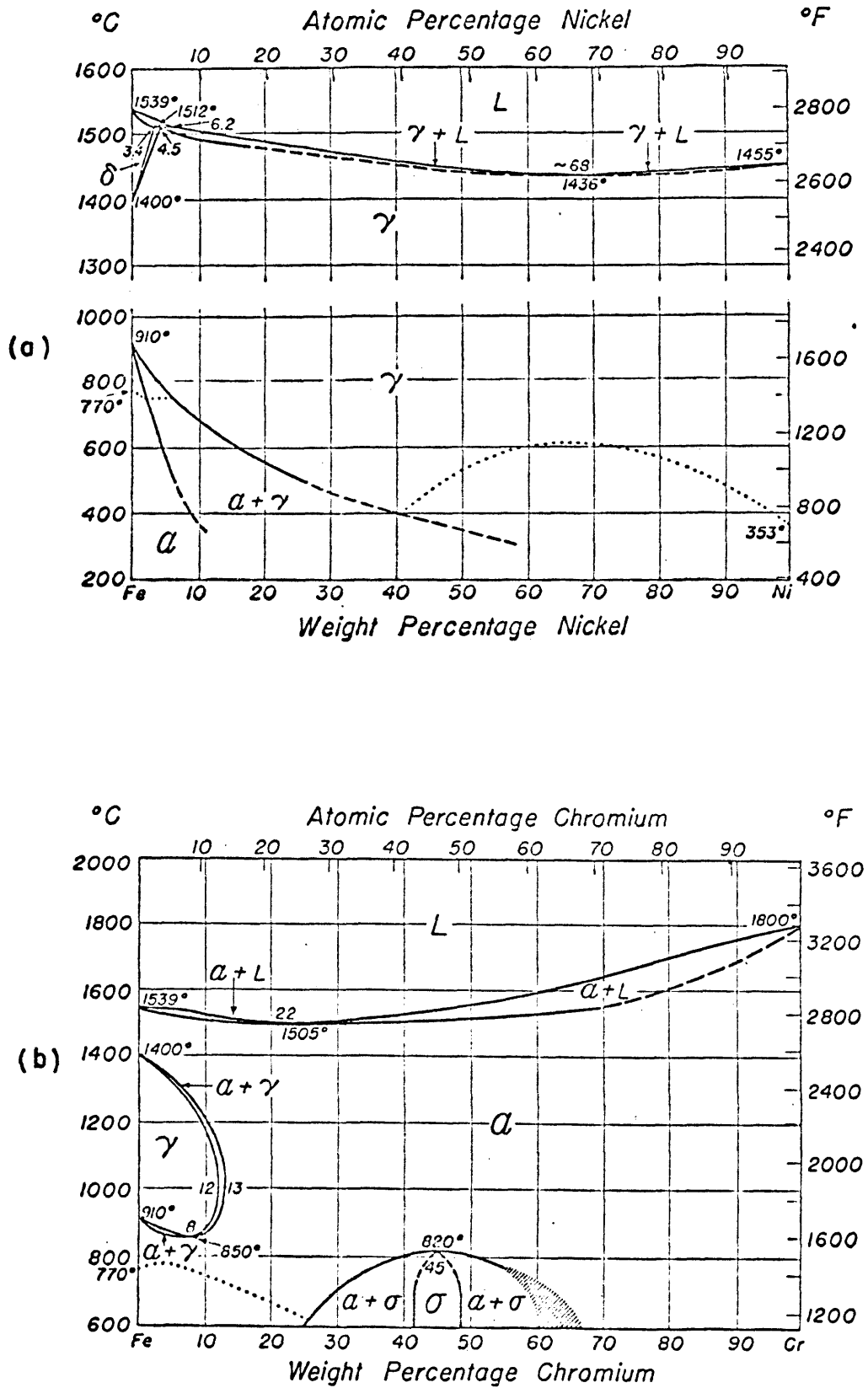


Figure 1 - Constitution Fe-Ni and Fe-Cr binary alloys.
 (Metals Handbook¹)

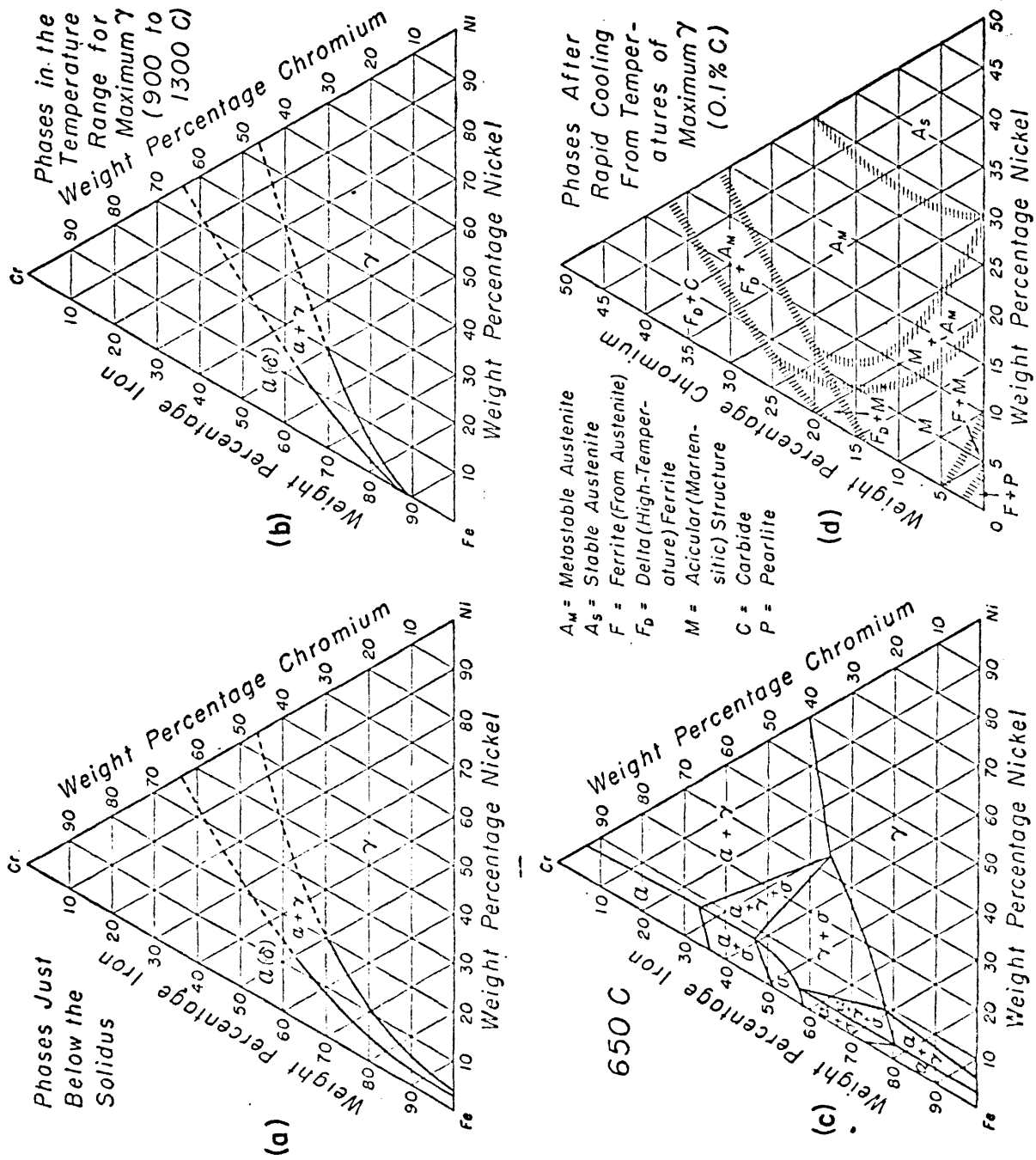


Figure 2 - Phase relationships in the Fe-Cr-Ni ternary system.

stabilizing power of the chromium but at the same time reducing the free carbon, a powerful austenite stabilizer.

Figure 2(d) gives a more valuable picture of the phases which may be observed in a commercial alloy at room temperature. In this case the alloys contain 0.1% carbon in addition to Fe, Cr, and Ni. Most alloys of commercial interest fall in or near the region labeled metastable austenite. All of the austenite present in the room temperature structure is not stable and in fact the austenite will partially transform to a body-centered cubic structure by cold working it at room temperature or by exposing it at subzero temperatures. This is a diffusionless transformation of the martensitic type.²

Structure and Properties. The structure of austenite is face-centered cubic. Because the atoms of the face-centered cubic austenite structure are more closely packed than those of the body-centered cubic ferrite phases, austenite is inherently more resistant to creep than is ferrite. Indeed, practically all of the high strength, high temperature steels presently used have austenitic matrices.³ The austenitic stainless steels are also used extensively for applications in various corrosive media and at cryogenic temperatures where brittle behavior of the body-centered structures is a detriment.

Ferrite

Depending upon bulk alloy composition, ferrite forms in

some nominally austenitic alloys during solidification. Ferrite observed in the microstructure of austenitic stainless steels at room temperature is generally labeled "delta" ferrite and is related to the allotropic transformation of iron from face-centered cubic to body-centered cubic above 2535^oF. This high temperature phase is retained upon cooling to room temperature and does not undergo the intermediate transformation to austenite.

Occurrence. As suggested by figure 2(a), formation of delta ferrite upon solidification of an alloy is a function of the bulk composition of the alloy. Because of coring, weld deposits or castings generally contain a greater amount of ferrite than homogenized wrought alloys of the same composition. A structural diagram for stainless steel weld metal was developed by Schaeffler⁴ and is shown in figure 3. This diagram is widely used to predict the structure of as-deposited stainless steel welds. The various minor alloying elements normally present are grouped as chromium or nickel equivalents according to their relative power as ferrite or austenite stabilizers as indicated.

Properties. The role of delta ferrite in reducing the hot cracking of austenitic stainless steel weld deposits and castings is well established.⁵ Through extensive review of the literature and experimental work, Hull⁶ concluded that austenitic stainless steel alloys containing 5 to 10% delta

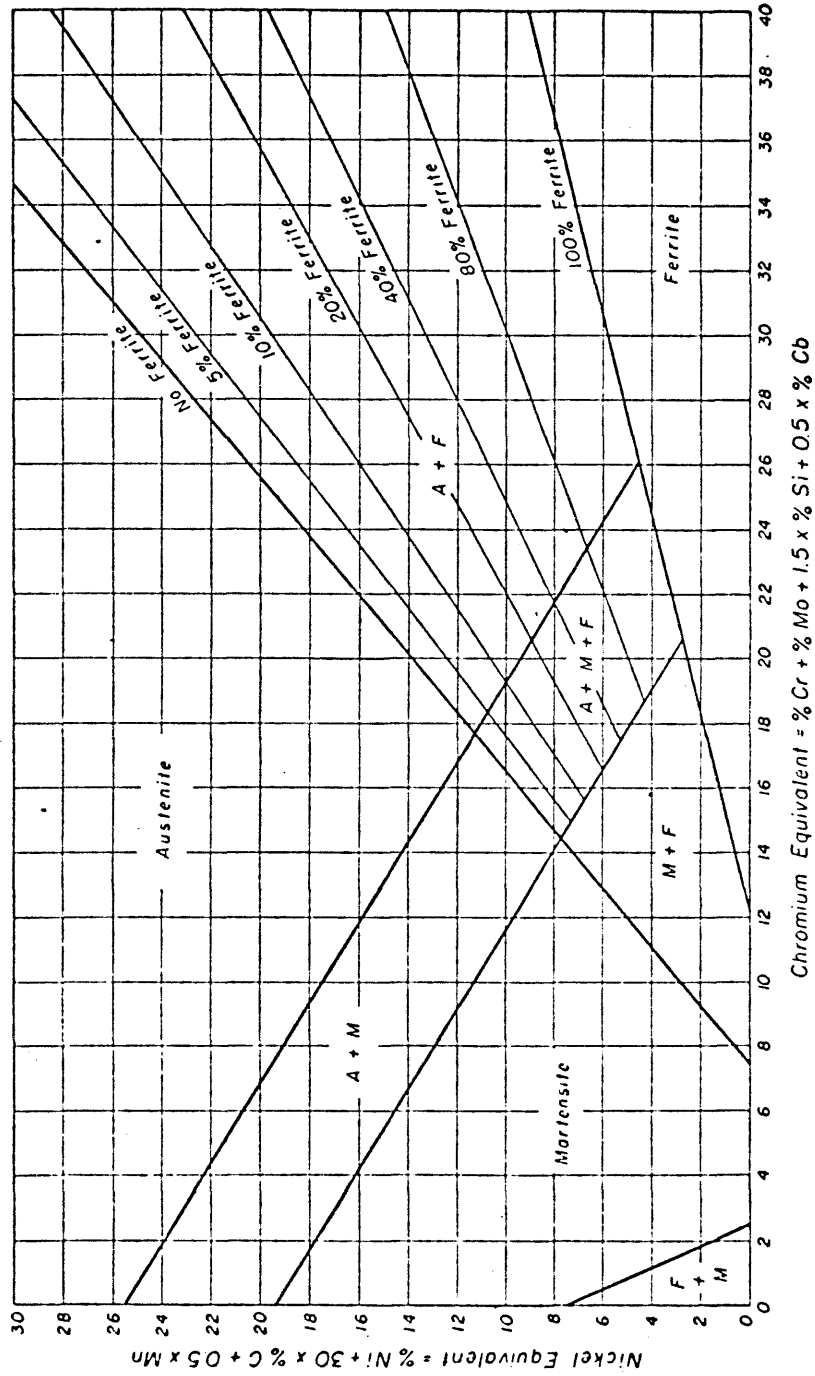


Figure 3 - Constitution diagram for stainless steel weld metal. (Schaeffler⁴)

ferrite in the as-cast microstructure are the most resistant to hot cracking. He postulated that the beneficial effect of delta ferrite results from the lower interfacial energy of an austenite:ferrite boundary than an austenite:austenite boundary. The austenite grain boundaries are wet by the last traces of liquid whereas the boundaries between austenite and ferrite are not wet and can sustain the contraction stresses imposed during cooling through the solidification range.

The yield point and tensile strength of austenitic stainless steels is generally increased by the presence of some ferrite in the microstructure, however creep strength at elevated temperatures is decreased. The presence of ferrite is detrimental to many hot-and-cold forming processes.⁵

From the microstructural standpoint, delta ferrite plays an important role in the precipitation of additional secondary phases. These relationships will be shown presently.

Carbides

Economic processing of commercial alloys results in all stainless steels containing some carbon. In the austenitic grades the amount of carbon generally ranges from about 0.08% max in the corrosion resistant alloys up to 0.25% max in the heat resistant alloys. Some of the characteristics and effects of the carbide phase which may form will be discussed.

Occurrence. Carbon shows a great affinity for chromium. Iron-chromium carbide of the type $M_{23}C_6$ will readily form

in austenitic alloys held in the temperature range of 900-1600^oF. This carbide contains a minimum of 70% chromium by weight.⁷ The carbide phase precipitates preferentially first at the ferrite boundaries if ferrite is present in the microstructure. This is evidently because of the higher chromium content in ferrite than in austenite. Subsequent precipitation is found along the austenite grain boundaries and finally within the grains, depending upon time at temperature.

Effects. Intergranular attack of austenitic stainless steels is usually associated with chromium carbide precipitation at the grain boundaries. The most widely accepted theory of intergranular corrosion in these alloys involves the formation of a zone adjacent to and including the grain boundaries which is depleted in chromium. This zone is thus less resistant to attack in corrosive media.⁸

In alloys containing greater than 0.15% carbon, a continuous network of carbides may surround each grain after exposure in the carbide precipitation temperature range. The ductility and toughness of these alloys may be substantially reduced because of the lack of cohesion between the grains.⁵

The Sigma Phase

The occurrence of sigma phase in austenitic stainless steels is of importance because of its generally deleterious effects upon mechanical and corrosion properties of these alloys. Because the factors affecting the precipitation

of sigma phase will form the central theme of this study, the literature pertaining to this subject will be reviewed in some detail.

The sigma phase was first observed by Bain and Griffiths⁹ in 1927 during a systematic study of a series of iron-chromium-nickel alloys. Since that time hundreds of investigators have published studies on different aspects of the subject. Interest in sigma phase warranted an A.S.T.M. symposium¹⁰ on the "nature, occurrence, and effects" of sigma phase held in 1950. Lena¹¹ produced a review of the work on sigma phase and its effect on commercial alloys in 1954 and a detailed review of the research on the structure, occurrence, and properties of sigma phase was provided by Hall and Algie¹² in 1966.

Physical Characteristics. Bain and Griffiths⁹ observed a very hard and brittle phase which showed hardness levels up to 68 Rockwell C by their measurements. This hardness and its embrittling effect on the steels in which it is found remains the outstanding characteristic of the sigma phase. Other less important physical characteristics include sigma's non-magnetic character and its low electrical resistivity.¹²

Structure. Because of its characteristic diffraction pattern, which is greatly different from patterns of other phases present in stainless steels, identification of sigma phase by x-ray analysis was used long before investigators

resolved the actual crystal structure of the phase. Menezes, Roros, and Read¹⁰ are credited¹¹ with establishing the true tetragonal symmetry and complex 30-atom unit cell of sigma phase. Structural factors such as ordering, electronic structure, defect structures, and atomic coordination in the sigma phase have been the subject of numerous studies and are summarized by Hall and Algie.¹²

Occurrence. The sigma phase has been positively identified in at least 40 binary systems and 30 ternary systems. Sigma phase forms in binary alloys of the transition metals, one component being from Group V_A or VI_A and the other from the First, Second, or Third long Period. One of the two metals is body-centered cubic while the other is face-centered cubic or hexagonal close packed in at least one of its allotropic forms.¹² Beyond this there seems to be no generalities which apply with consistency.

In this study we will be concerned with the sigma phase as it occurs in the Fe-Cr-Ni ternary system. As will be seen presently, the behavior of the sigma phase in this system will be altered drastically by small additions of other alloying elements.

The Sigma Phase in Commercial Alloys. Because of the extremely slow rate of transformation of sigma in annealed alloys of high purity, the existence of sigma phase was doubted for several years following its discovery by Bain and Griffiths in 1927. In commercial alloys, however, even annealed specimens may show sigma transformation at relatively short time

with proper composition and thermal treatment. This discussion will be limited mainly to alloys based on the Fe-Cr-Ni ternary system and showing a fully austenitic or duplex austenitic ferritic structure at room temperature. The ferritic Fe-Cr alloys will be discussed first to provide a starting point from which to move into discussion of the Fe-Cr-Ni system.

Sigma in Ferritic Fe-Cr Alloys. Figure 4 is a portion of the Fe-Cr phase diagram showing the limits of sigma phase formation in pure alloys as derived by A.J. Cook and F.W. Jones.¹³ Alloys were of very high purity and equilibrium was obtained by cold working the samples prior to aging. Regarding the effect of cold work, it was found that filings of a 53% chromium alloy reached equilibrium in two days at 1330°F whereas a bulk sample of the same alloy had not started to transform after 37 days.

A comparison of the phase boundary for high purity alloys determined by Cook and Jones¹³ and commercial alloys with less than 0.1% carbon was made by Shortseleeve and Nicholson¹⁴ and is shown in figure 5. As may be seen, the effect of small amounts of impurities can make the formation of sigma more favorable. The effects of small additions of various alloying elements on the formation and stability of sigma phase in Fe-Cr alloys are known through investigations of ternary systems and are summarized by Hall and Algie.¹² In general, the "ferrite stabilizers" (molybdenum, tungsten, vanadium,

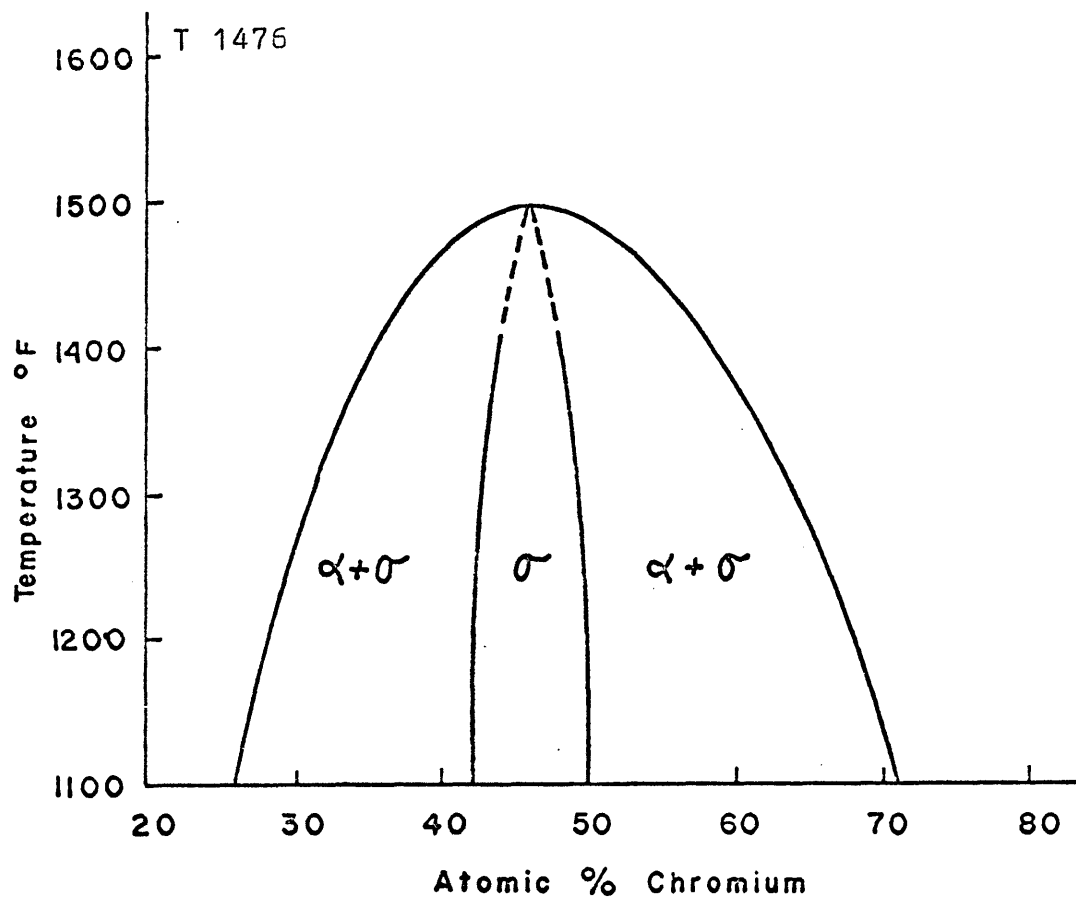


figure 4

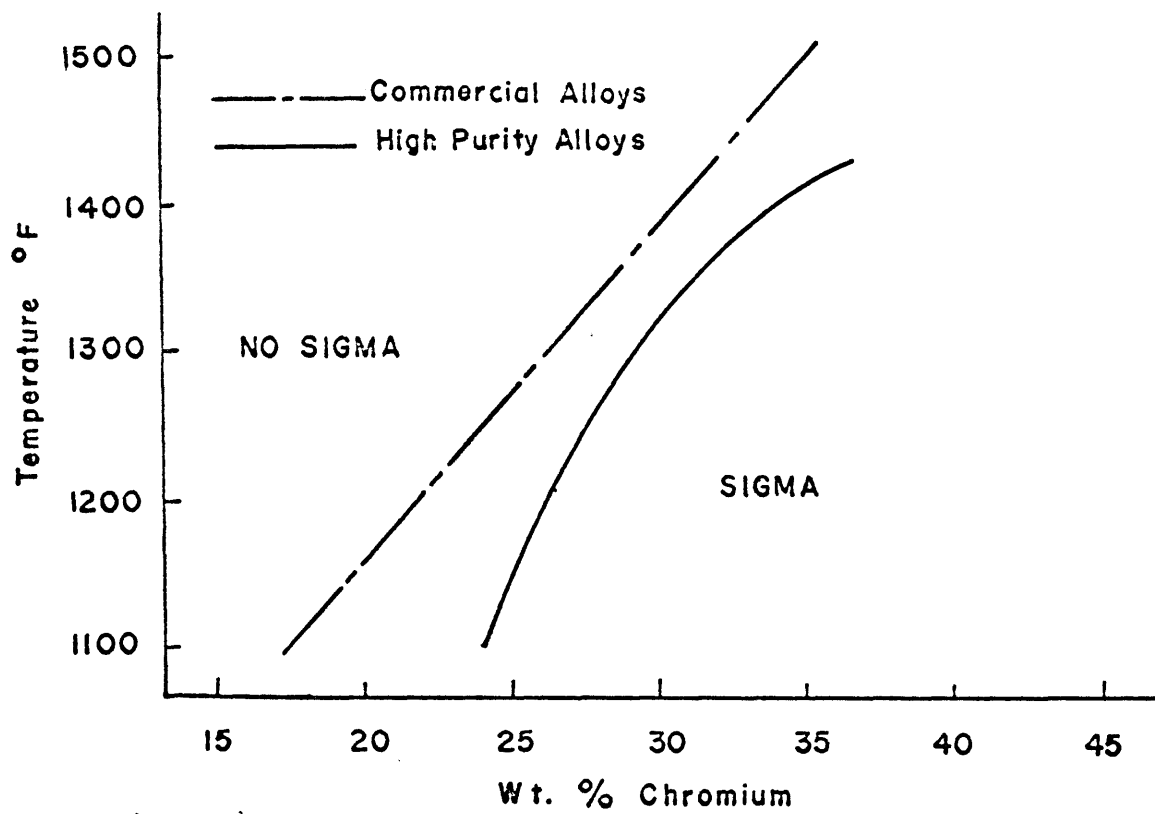


figure 5

titanium, and niobium) promote sigma formation. Although silicon does not form sigma phase in binary systems with the transition metals, it stabilizes the sigma phase in Fe-Cr-Si alloys over a large range of composition and at temperatures as high as 1830°F. In addition to stabilizing the range of composition of sigma, these elements have a marked positive effect on the rate of formation. Austenite stabilizers, notably nickel and manganese, may expand the range and rate of formation when present in amounts smaller than about 4%. However, when larger amounts are present, austenite forms and these elements then exert a negative effect on sigma formation. Carbon is thought to reduce sigma formation by lowering the effective chromium content through carbide formation.

Sigma in Austenitic Fe-Cr-Ni Alloys. The formation of sigma in austenitic stainless steels has been the subject of intense study in the past, principally because of the application of these steels in high temperature service. Although the limits of sigma phase formation in Fe-Cr-Ni alloys of high purity has been studied extensively,¹⁵ this information is of limited value in prediction of sigma phase formation in commercial alloys, particularly when the alloy composition lies close to a phase boundary. In such alloys, variation of composition within allowable limits may be sufficient to cause formation of sigma. A diagram for Fe-Cr-Ni alloys of commercial purity derived by Nickolson, Samans, and

Shortsleeve,¹⁶ is shown in figure 6. This is an isothermal section at 1200°F and shows the relative location of a number of important A.I.S.I. stainless steel compositions.

A large volume of information is available on the formation of sigma in commercial steels. Certainly enough data are available to accurately predict sigma phase in any important alloy and thereby avoid it by adjustment of alloy composition. Beyond this, however, there is little general agreement on the details surrounding the nature of sigma phase formation. A few of the important observations of previous investigators will be considered in the following paragraphs.

The Kinetics of sigma phase precipitation in a number of commercial Fe-Cr-Ni alloys was reported by Tisinai et al.¹⁷ These investigators studied the rate of transformation in the region of 1000 to 1600°F and found that the time-temperature-transformation curves followed the familiar C-shaped behavior which is characteristic of nucleation and growth processes. The temperature of the maximum formation rate generally increased with increasing content of sigma forming elements.

It is generally agreed that a small percentage of ferrite in an austenitic matrix will greatly enhance the rate of sigma formation. Reasons suggested for this effect include the higher alloy content (sigma formers) of ferrite;¹⁸ greater atomic mobility in ferrite than in austenite;¹⁹ relationship of the crystallographic structures of austenite, ferrite, and sigma;^{19, 20} and preferential precipitation of carbides in

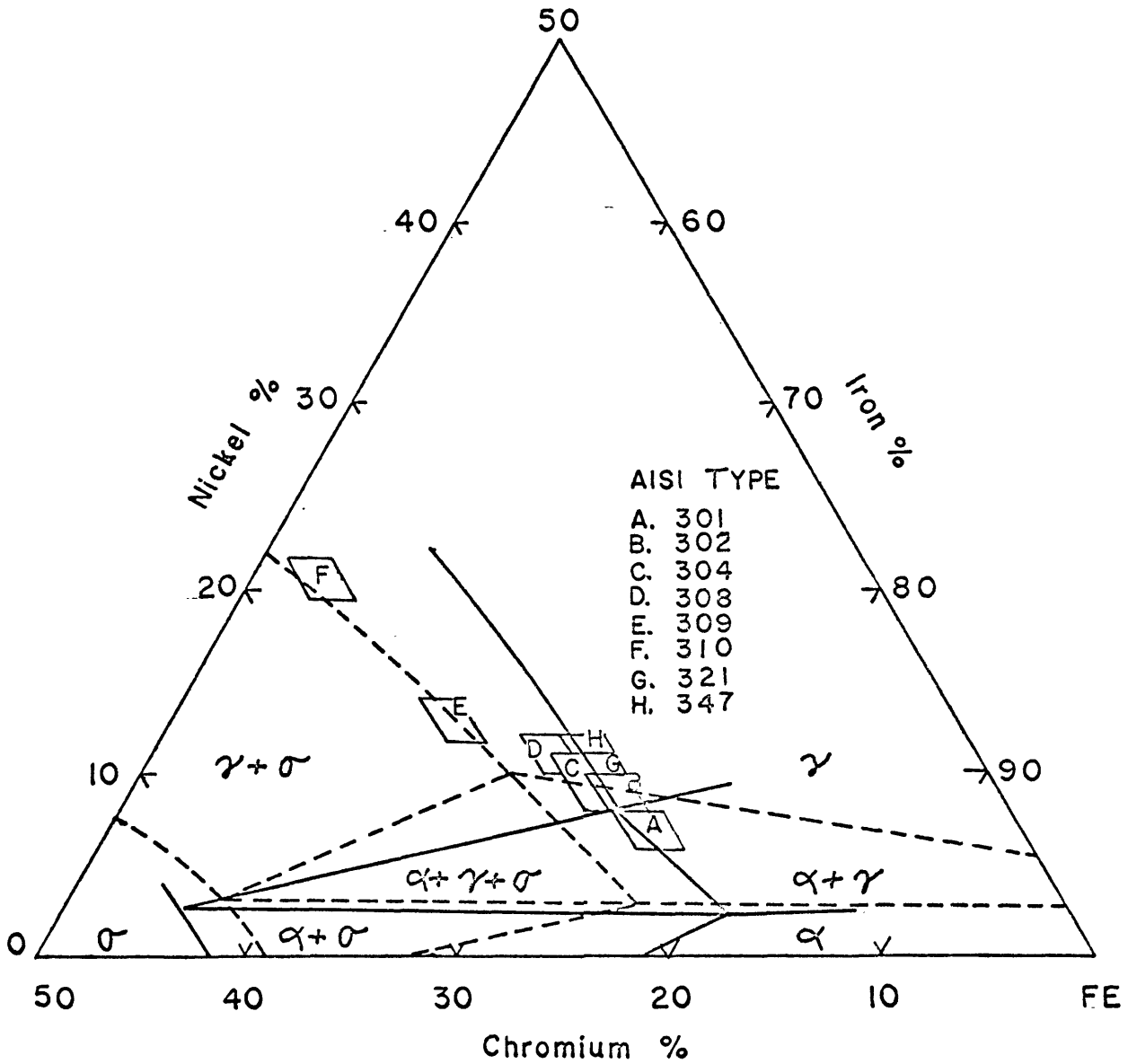


figure 6

Nicholson, Samans, and
Shortsleeve, Trans ASM, v. 44, p. 609.

———— Commercial Purity
 - - - - - High Purity

ferrite thereby creating preferred nucleation sites or concentration of sigma forming elements.^{19,20-23} Sigma phase precipitated from ferrite in duplex structures has been reported in "as cast" samples. By contrast, typical times for sigma formation in annealed fully austenitic structures are 500-1000 hr at the maximum rate.

The effect of carbides on the nature of sigma formation is particularly disputed in the literature. Albritton and Kadlec²¹ concluded that for rapid sigma formation there must necessarily be prior carbide precipitation. Blenkinsop and Nutting²⁵ found that if carbide precipitated before sigma, the rate of formation of sigma was retarded. Recent studies using electron microscopy have failed to confirm nucleation of sigma on carbide particles.^{24,25}

It seems appropriate to mention some of the pertinent observations of sigma phase studies which have been applied directly to welding problems. Albritton and Kadlec²¹ observed slight sigma phase formation in a type 309 filler metal deposited on $1\frac{1}{4}\text{Cr}-\frac{1}{2}\text{Mo}$ steel plate which had been stress-relieved for 2 hr at 1350^oF and then furnace cooled at 100 deg/hr. Complete delta ferrite to sigma transformation was observed after 93 hr at 1350^oF. Creamer, Rosalsky, and Leonard²⁶ identified sigma in a type 347 stainless steel weldment which had been held at 1340^oF for 3 months. The weld metal sigmatized to a greater extent than the base metal because of composition and ferrite content, according to the

authors. Daemen and Dept²⁷ observed complete transformation of ferrite to sigma in stainless steel strip cladding using type 316 L filler metal after reheating to 850^o C for less than 5 minutes.

Effect of Sigma Phase on the Properties of Alloys. The affect of sigma phase on the mechanical properties of common Fe-Cr-Ni alloys is well established and is reviewed in detail by Lena.¹¹ It appears characteristic that sigma exerts a greater influence on impact strength than any other property. Reports of a marked decrease in impact strength without major changes in other properties are common. In particular, hardness and tensile strength of sigmatized steels are often not affected or only slightly altered. However, significant increase in strength may be produced in many steels by sigma formation. This generally requires a fine distribution of the sigma phase as would be expected in fully austenitic or fully ferritic alloys. Sigma-strengthened alloys have found limited application in high temperature service where resistance to shock is not a requirement. Sigma may increase creep strength of stainless steels for short time applications, but in long time applications sigma decreases creep strength.

Corrosion resistance of sigmatized stainless steel is impaired in nitric and sulfuric acids, especially when the sigma is present as a fine dispersion. Increased corrosion rates in other media have not been established. The effect of sigma on corrosion resistance has been attributed to a

chromium depletion mechanism much the same as that associated with carbide precipitation^{11,23} and to a stress-corrosion effect caused by high strain energies in the neighborhood of sigma precipitates.²⁸

EXPERIMENTAL PROCEDURE & RESULTS

The experimental procedure and observed results are related below. Discussion of these results will be reserved for the next section.

Selection of Alloys

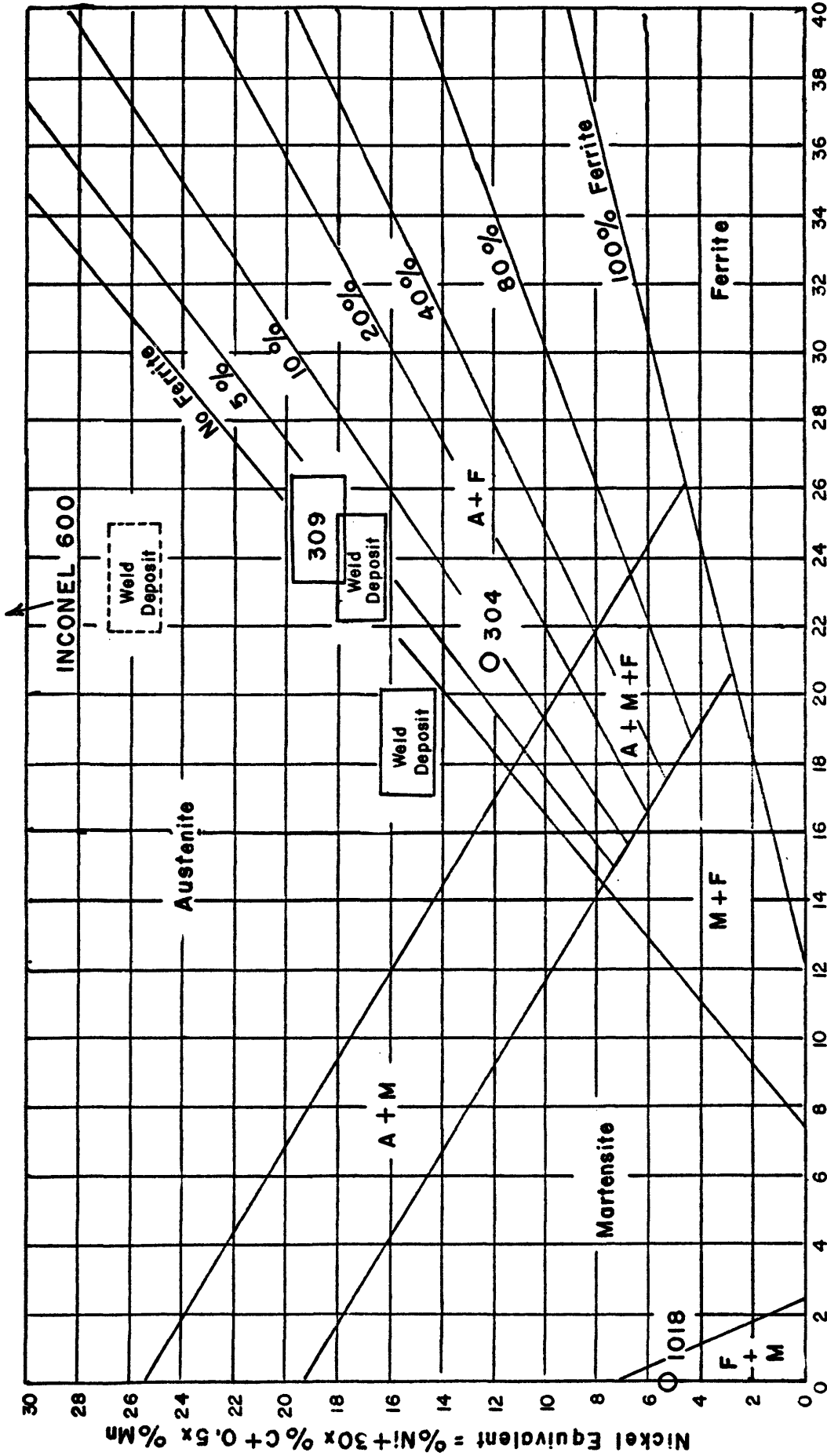
Specified compositions for the filler metal and base metals are shown in table 1.^{29,30}

Filler Metal. The filler metal alloy chosen for this study was AWS-ASTM type ER 309 supplied as 1/16 in. bare wire. This choice was made to provide the likelihood that the as-deposited microstructure would exhibit a duplex type structure when deposited on at least one of the available base materials. The composition envelope for the ER 309 filler metal is plotted on the Schaeffler diagram shown in figure 7.

Base Material. The plate materials used for this investigation were $\frac{1}{4}$ in. AISI type 304 stainless steel, $\frac{3}{16}$ in. AISI type 1018 plain carbon steel, and $\frac{1}{8}$ in. Inconel 600 alloy. The center points of the composition envelopes (except the Inconel) are plotted in figure 7. To estimate the as-deposited filler metal composition, dilution-direction lines may be drawn from the filler metal composition to the base metal composition. The as-deposited filler metal composition

Alloy Designation	Composition limits by weight					
	C	Mn	Si	Cr	Ni	Fe
<u>Filler Metal</u>						
ER 309	0.12 max	1.0- 2.5	0.25- 0.60	23.0- 25.0	12.0- 14.0	bal
<u>Base Metals</u>						
304	0.08 max	2.0 max	1.0 max	18.0- 20.0	8.0- 12.0	bal
Inconel 600	0.15 max	1.0 max	0.50 max	14.0- 17.0	72.0 min	6.0- 10.0
1018	0.15- 0.20	0.60- 0.90	0.10- 0.30			bal

Table 1 - Nominal compositions of filler and base metals.



Chromium Equivalent = %Cr + %Mo + 1.5x%Si + 0.5x%Cb

Figure 7 - Estimation of weld deposit composition and structure using the Scheffler diagram.

is then shifted from the undiluted filler metal composition along the line a proportional distance equal to the amount of observed dilution of the filler metal by the base metal. The average dilution for all weld deposits was observed to be 32% with a range from 25% to 37%. Dilution was measured by making photomicrographs of transverse sections of the weld deposits and then cutting out and weighing the portions of the pictures corresponding to the diluted and undiluted portions of the weld deposit. Such a picture is shown as figure 8.

Welding

The welding for this investigation was done using an automatic gas-metal arc-welding process with an Airco Hornet constant potential welder. Operation of the machine is such that arc travel speed and wire feed speed may be adjusted independently. The welding current and potential which results from welding at a given travel speed and wire feed is automatically fixed and not adjustable. For this study a travel speed of 36 in./min and wire feed of 250 in./min were used. This resulted in a welding current of 300 amp with a potential of 26 v. On this basis, energy input was 13,000 joules/in.

The base materials were cut into pieces approximately $2\frac{1}{2}$ in. x 6 in. and the weld bead was deposited along the centerline in the long direction. The shielding gas used was argon-2% oxygen at a flow rate of 40 cu ft/hr.

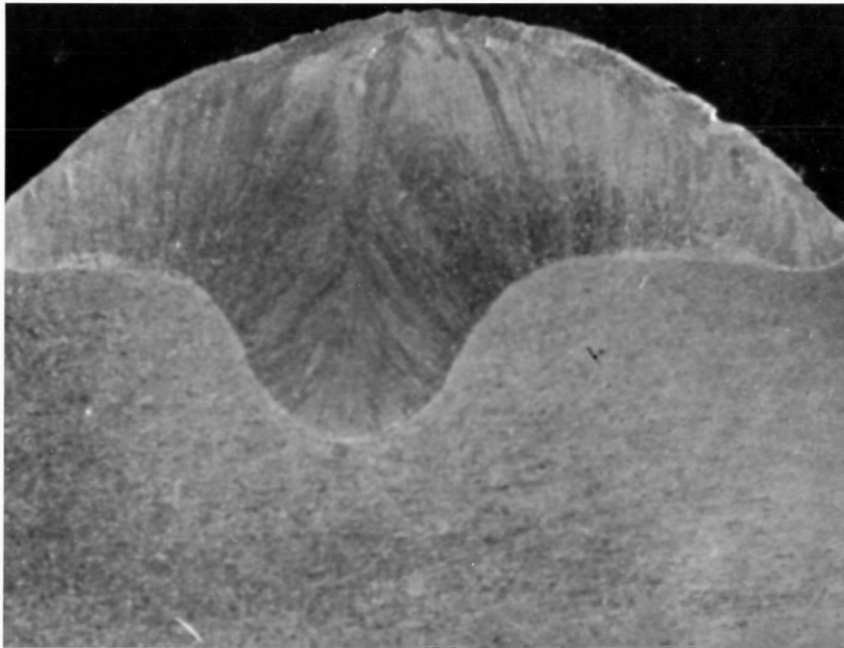


Figure 8 - Photomicrograph of ER 309 filler metal
on type 304 stainless steel base.

Heat Treatment

After welding, the deposited weld was removed from the plate by making cuts along each side of the bead, thereby retaining only the weld deposit and the base material directly under it. The weld deposit was then sliced into pieces about $\frac{1}{4}$ in. long by cutting perpendicular to the welding direction. These specimens were then examined in the as-welded condition or subjected to two types of heat treatment.

Solutionizing Treatment. Approximately half of the specimens were subjected to a solutionizing or solution annealing heat treatment. This heat treatment is a standard commercial practice, the main purpose of which is to dissolve chromium carbides which may form during welding or hot-working of austenitic stainless steels. The treatment used consisted of heating the specimens at 2000^o F for 1 hr followed by an agitated water quench.

Aging Treatment. A second heat treatment to which all specimens were subjected consisted of an aging treatment at 1350^o F. This temperature was chosen based on the temperature of maximum sigma phase formation found by Tisnai et al¹⁷ for a wrought type 309 stainless alloy. Aging times ranged from 20 min to 500 hr. Aging treatment was followed by an agitated water quench in each case.

All heat treatments were conducted in small laboratory type electric muffle furnaces. No protective atmosphere was used.

Metallography

As welded and heat treated specimens were prepared for observation by optical microscopy as described below.

Preparation. Specimens were mounted in Bakelite mounting material using a 1-in. diameter mold. All specimens were ground and polished by the same procedure. This consisted of first wet grinding to obtain a plane surface, and then dry grinding successively on no. 1,0,00 and 000 polishing papers. Polishing of the specimens was accomplished by first rough polishing on canvas using 5.0 micron alumina as an abrasive followed by final polishing on Microcloth using 0.5 micron alumina. Because the austenitic stainless steel surface tends to flow easily during polishing, it was necessary to etch each specimen twice using a solution consisting of 5g FeCl_3 , 50 ml HCl , and 100 ml H_2O for 30 sec and repeating the rough and final polishing steps. After a final etch of 10 sec in the above solution, the specimens were given a final polish yielding a surface suitable for microscopic examination.

Etching. The etchants used in this investigation are summarized in table 2. These etchants can be categorized generally as: 1) inorganic acids in water or alcohol used by immersion or electrolytically, 2) organic acids in water used electrolytically, or 3) aqueous alkaline ferricyanide solutions used by immersion or electrolytically. The general structure and secondary phases of the weld deposits studied

REAGENT	COMPOSITION	USE
Oxalic acid	Oxalic acid... 10g H ₂ O.....100ml	Used electrolytically with specimen as anode. Carbides, sigma, and general structure revealed after etching for 5-30 sec at 3 v.
Chromic acid	CrO ₃ 10g H ₂ O..... 100ml	Sigma and carbides are attacked rapidly in less than 10 sec when etched electrolytically at 5 v with specimen as anode.
Kalling's reagent	CuCl ₂ 5 g HCl .. 100ml Ethyl alcohol.100ml H ₂ O100ml	Etching for 10 sec attacks ferrite, leaving austenite, carbides, and sigma unaffected. Light hand polish usually needed after etch to eliminate surface staining.
FeCl ₃ -HCl	FeCl ₃ 5 g HCl..... 50ml H ₂ O.....100ml	Etching 15-30 sec reveals general structure of austenitic stainless steels.
Murakami's reagent	Potassium ferricyanide. 10g KOH..... 10g H ₂ O.....100ml	All combinations attack and stain the sigma phase. Colors observed for sigma ranged from light blue to dark brown. These reagents were used by immersion and electrolytically at temperatures ranging from room temperature to the boiling point as described in the text.
a) Normal	Potassium ferricyanide. 20g KOH..... 20g H ₂ O.....100ml	
b) Double strength	Potassium ferricyanide. 50g KOH..... 50g H ₂ O.....100ml	
c) Concentrated	as (c) above, but with 10g Pot. ferr.	
d) Conc.(modified)		

Table 2 - Etching reagents employed.

were revealed by using these etchants alone or in series. For example, all of the possible microconstituents of the aged weld deposit could be revealed and identified by first etching in $\text{FeCl}_3\text{-HCl}$ to reveal the general structure, re-polishing and etching lightly in Murakami's reagent to reveal only the carbides, and finally etching in chromic acid, which rapidly attacks both the carbides and sigma phase.

At this point it should be noted that the weld deposits on the plain carbon steel and Inconel 600 base materials showed, upon etching, a fully austenitic structure as predicted by the Schaeffler diagram. Preliminary investigation showed no significant change in microstructure for these deposits during the solutionizing treatment and only a slight amount of carbide precipitation for long holding times during the aging treatment. In addition, the weld deposits showed a columnar structure of relatively large grain size, resulting in a somewhat uninteresting microstructure from the standpoint of optical microscopy. Because the microscope was the primary tool available for this investigation and because the duplex structure of the welds deposited on the type 304 stainless steel were of a much more interesting nature in terms of transformation during heat treatment, further investigation of the fully austenitic weld deposits was abandoned in favor of a more concentrated effort in studying the transformation of the duplex structure.

Photomicrography. The heat treated weld deposits of ER 309 filler metal on type 304 stainless steel plate were studied thoroughly by optical microscopy. Representative photomicrographs of the observations made are shown on the pages to follow. All of the following photomicrographs are of specimens sectioned transverse to the welding direction.

Ferrite and sigma contents of several of the specimens used in this study were measured under the microscope using a point count technique. Thirty points in a 4 in. x 5 in. field were used. Counting was done at 1000X magnification and 25 randomly selected fields were counted in each case. The measurements showed an initial ferrite content of the as-welded deposit of approximately 30%. The amount of sigma phase found in the as-welded structure after aging at 1350° F for 24 hr was 17.7%. This agrees with a visual estimation that about 60% of the original ferrite was transformed to sigma after 24 hr at 1350° F. Ferrite content of the solution annealed specimen was measured to be 8.6%.

Other observations of the microstructure of these weld deposits which seem important but which did not lend themselves to photographic recording include:

1. Amount of ferrite which transformed to sigma upon aging progressed steadily with time at temperature for the as-welded specimens. Transformation of a small amount (less than 5%) of the ferrite was observed after 20 min at the aging temperature. An estimated 80% of the ferrite had transformed to

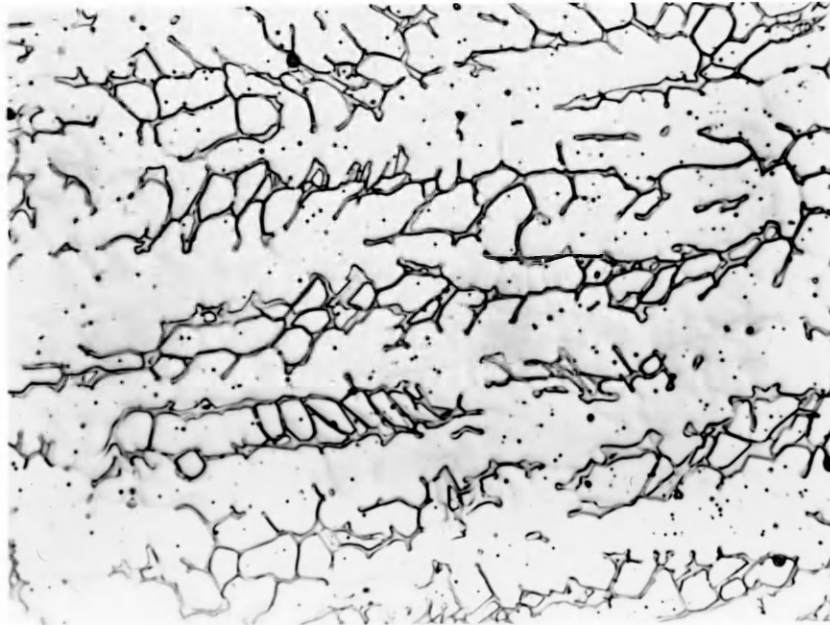


Figure 9 - Specimen in as-welded condition, 720X, etched electrolytically in oxalic acid at 3 v for 10 sec. A duplex austenite-ferrite microstructure with a dendritic solidification pattern is shown. The ferrite has solidified between the austenite dendrites.

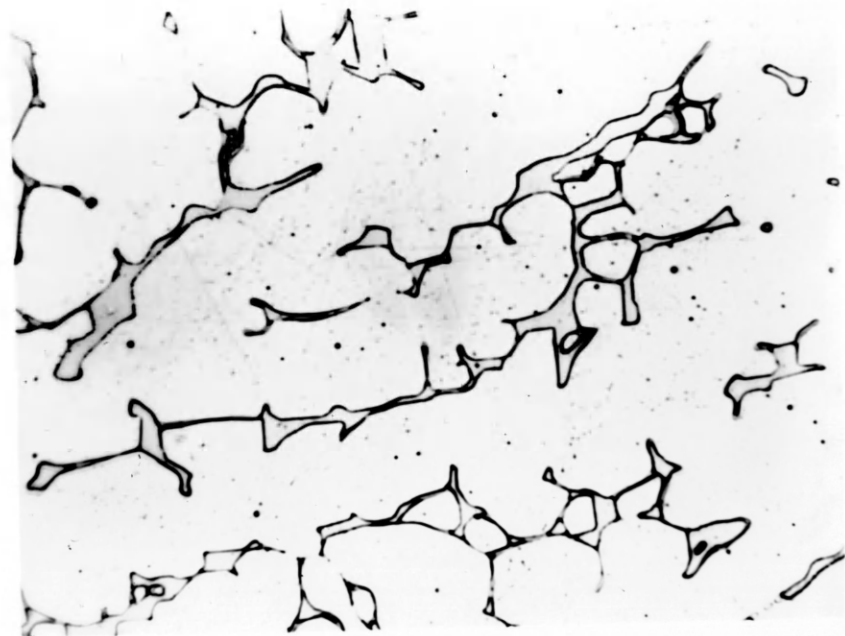


Figure 10 - Same specimen as figure 9, 1500X, etched in boiling double strength Murakami's reagent for 15 sec.



Figure 11 - As-welded specimen aged for 1 hr at 1350^o F, 1000X, etched in boiling strength Murakami's reagent for 15 sec. Specimen shows transformation of a small amount of ferrite to sigma phase.

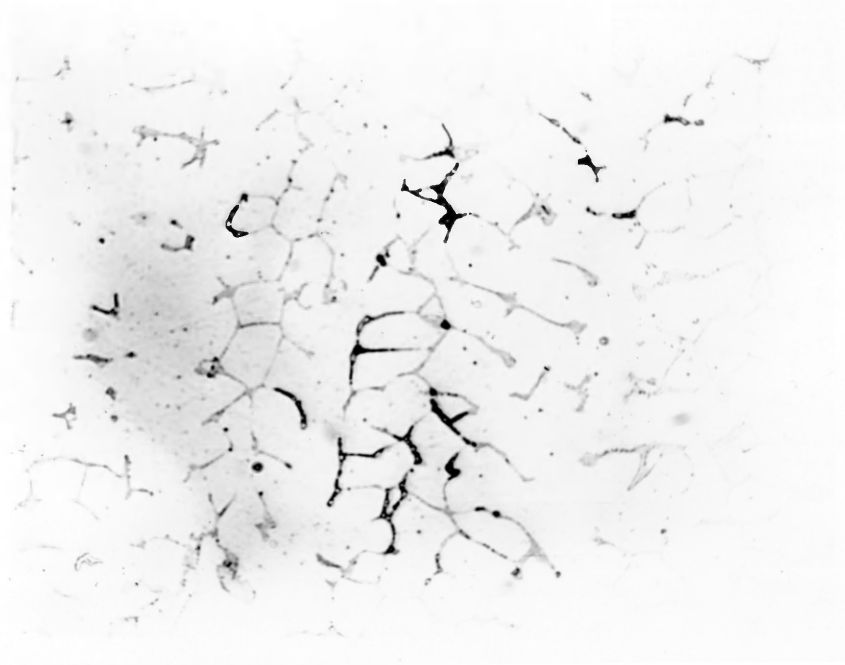


Figure 12 - As-welded specimen aged for 4 hr at 1350^o F, 1000X, etched in boiling double strength Murakami's reagent for 15 sec. Precipitation of sigma phase has progressed beyond that of specimen aged for 1 hr.



Figure 13 - As-welded specimen aged at 1350^o F for 24 hr, 1500X, etched in FeCl₃-HCl for 15 sec. Austenite, ferrite, sigma, and carbides are shown in the general structure.



Figure 14 - Same specimen as figure 13, 1500X, etched in boiling double strength Murakani's reagent to reveal the sigma phase. Sigma is the dark colored phase in this photomicrograph. In the microscope the phase appeared rich brown in color under white light.

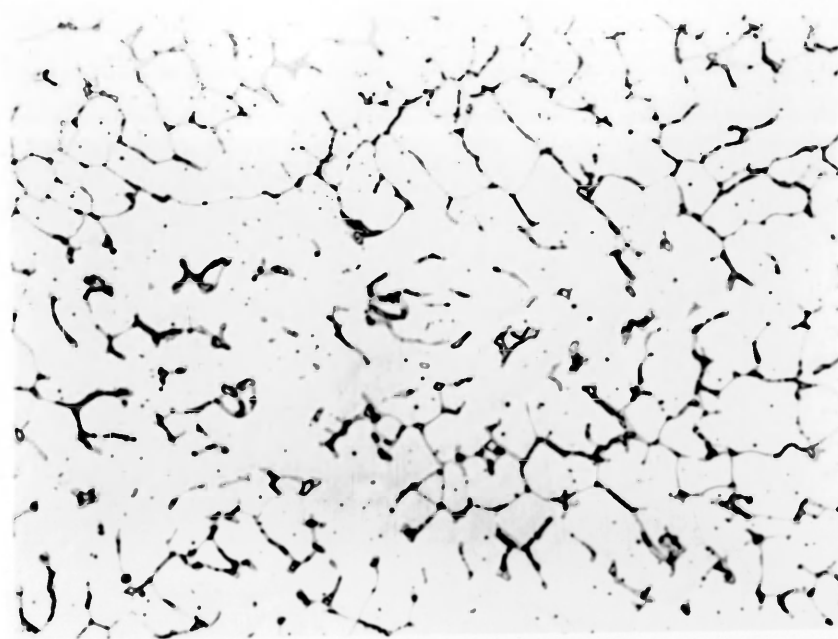


Figure 15 - As-welded specimen aged at 1350^o F for 24 hr, 720X, etched electrolytically in oxalic acid at 3 v for 10 sec. Degree of transformation after aging for 24 hr may be seen by comparing this photomicrograph with figure 9 which is the as-welded structure revealed by the same etchant and shown at the same magnification.

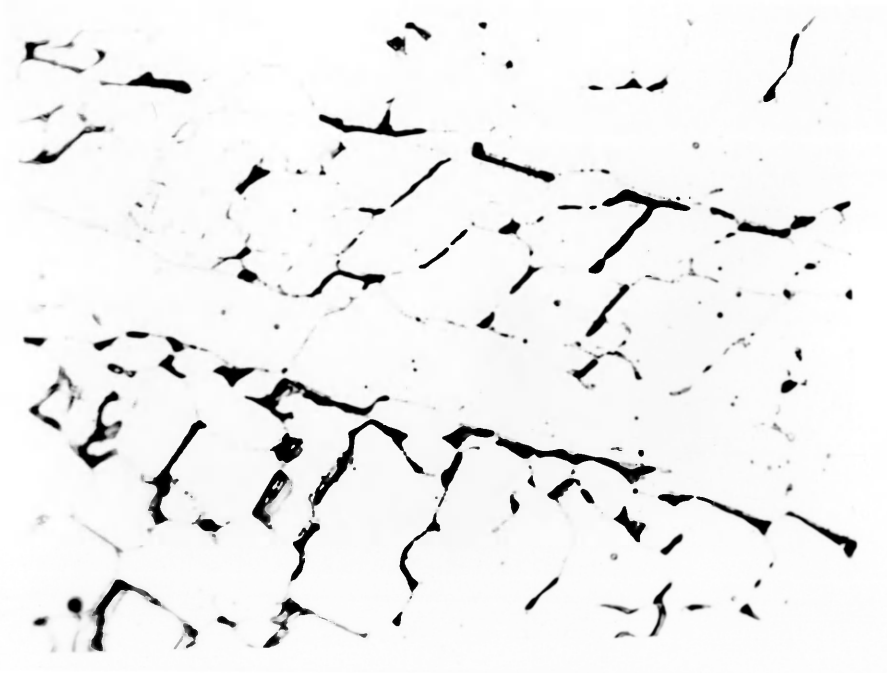


Figure 16 - Same specimen as figure 15, 1500X, electrolytically etched in chromic acid at 5 v for 5 sec. This etchant rapidly attacks sigma and carbides.

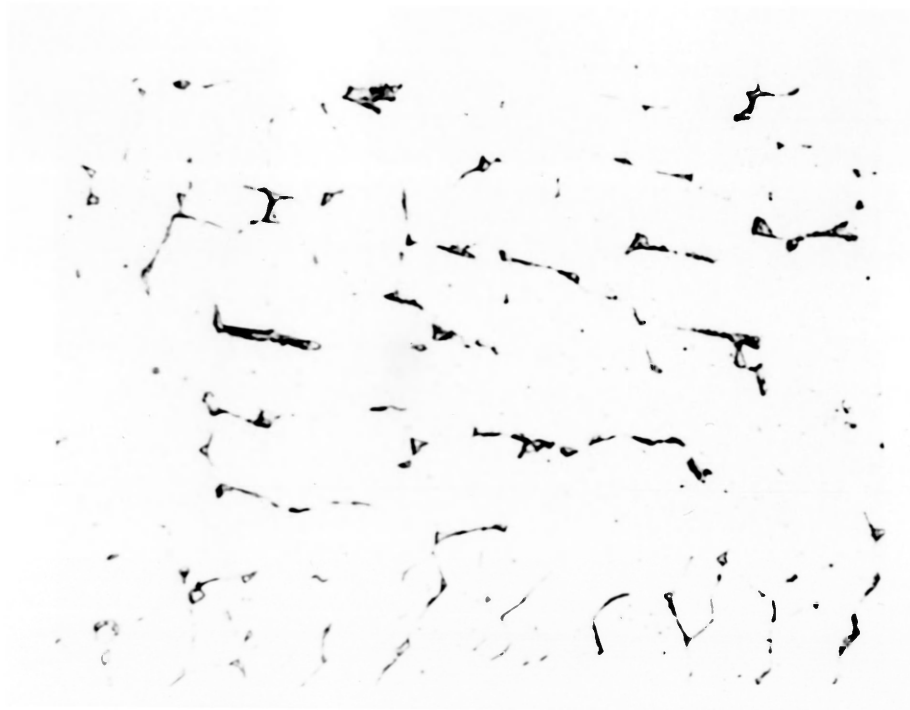


Figure 17 - As-welded specimen aged at 1350^o F for 24 hr, 1500X, etched in Kalling's reagent followed by a light polish. This etchant attacks only ferrite leaving austenite, carbides, and sigma unaffected. The decrease in the amount of ferrite as it transforms to sigma may be seen by comparing this photomicrograph with that shown in figure 10.

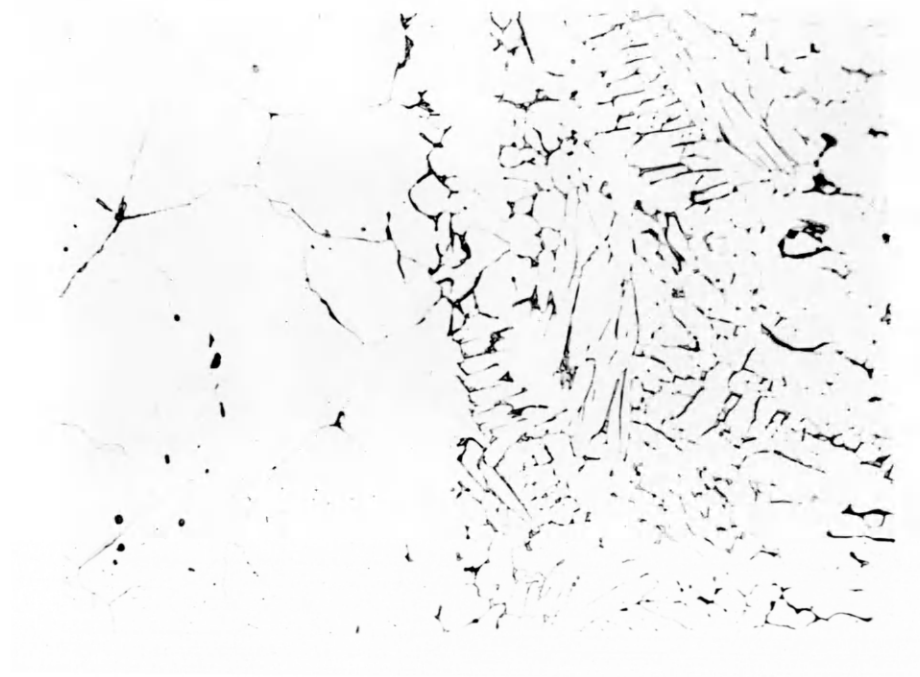


Figure 18 - As-welded specimen aged at 1350^o F for 24 hr, 500X, etched in FeCl₃-HCl for 15 sec. Weld-base metal interface is shown.

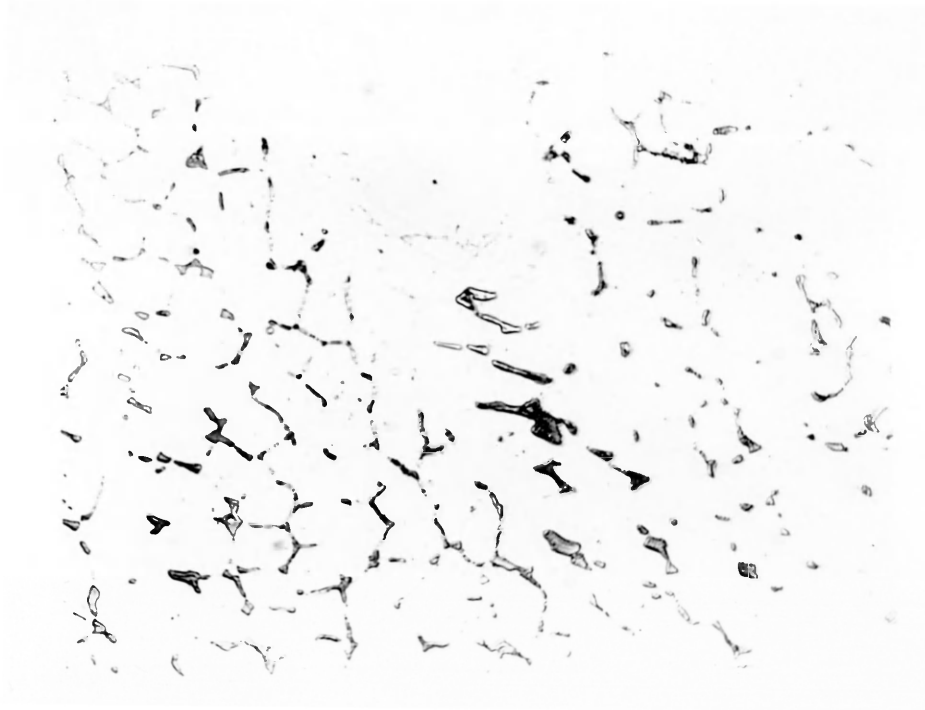


Figure 19 - As-welded specimen aged at 1350^o F for 100 hr, 1000X, etched in modified concentrated Murakami's reagent for 2 sec at 120^o F.

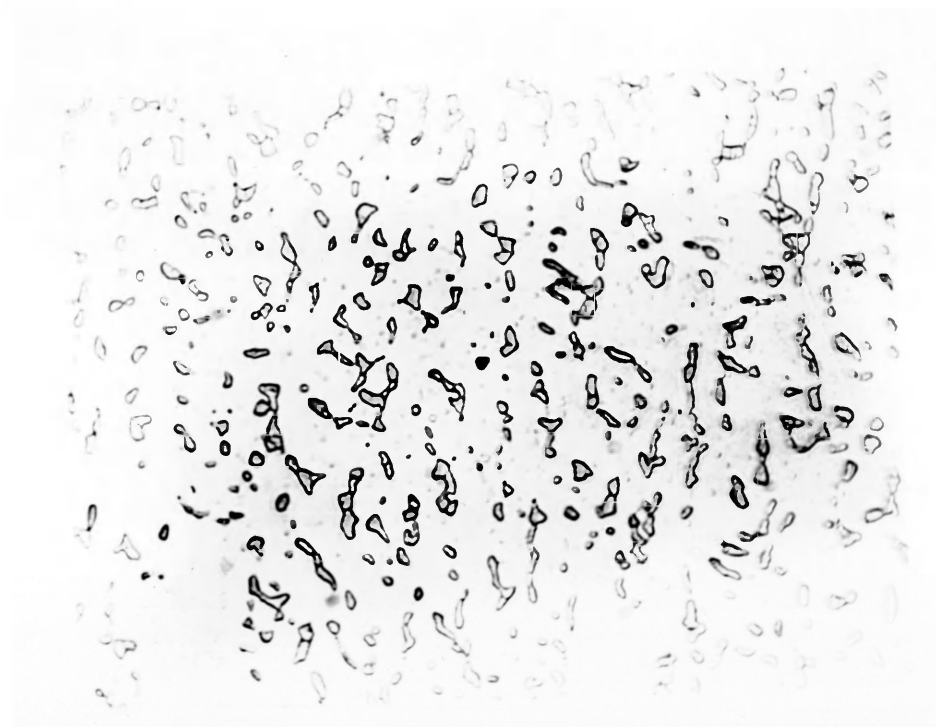


Figure 20 - As-welded specimen aged at 1350^o F for 500 hr, 1000X, etched in modified concentrated Murakani's reagent for 2 sec at 120^o F. The sigma phase appeared blue when viewed under white light. A tendency of the sigma phase to agglomerate after aging at 1350^o F for long periods of time may be seen.

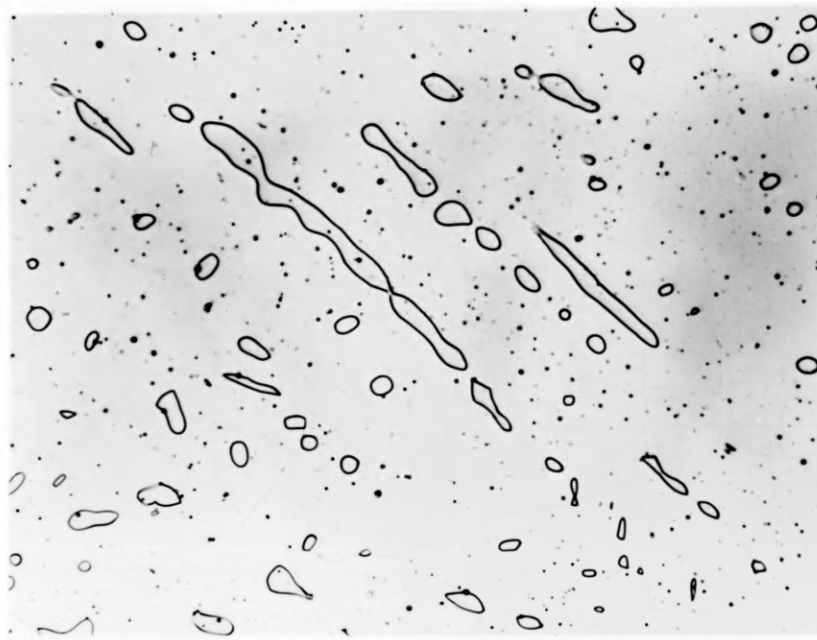


Figure 21 - As-welded specimen solutionized at 2000^o F for 1 hr followed by water quench, 720X. Etch is oxalic acid used electrolytically at 3 v for 10 sec. Comparison with figure 9 shows that the solutionizing treatment has agglomerated the inter-dendritic ferrite into relatively large pools bounded by smooth surfaces.

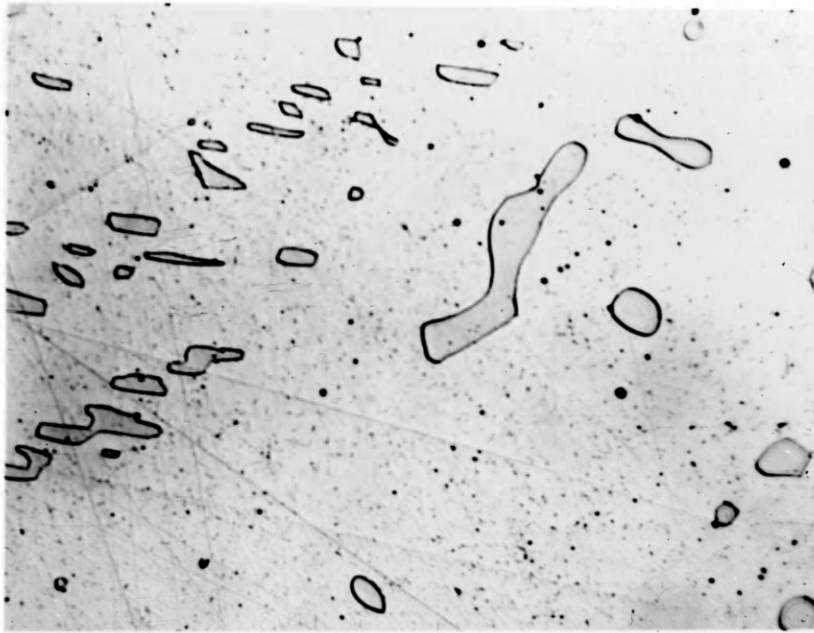


Figure 22 - Same specimen as figure 21, 1500X, etched electrolytically in Murakami's reagent for 5 sec at 1 v followed by immersion for 2 min in concentrated Murakami's reagent at room temperature. This etchant, which will reveal sigma and carbides, shows only the ferrite boundaries in this photomicrograph.

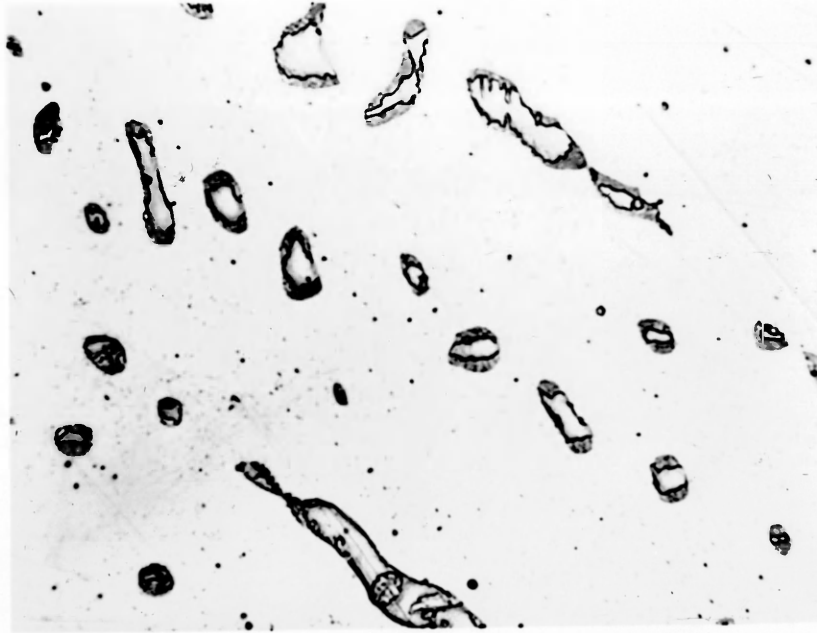


Figure 23 - Solution annealed specimen aged at 1350^o F for 20 min, 1500X, etched as in figure 22. Edges of ferrite areas have transformed into an apparently duplex product which can not be resolved in the microscope.

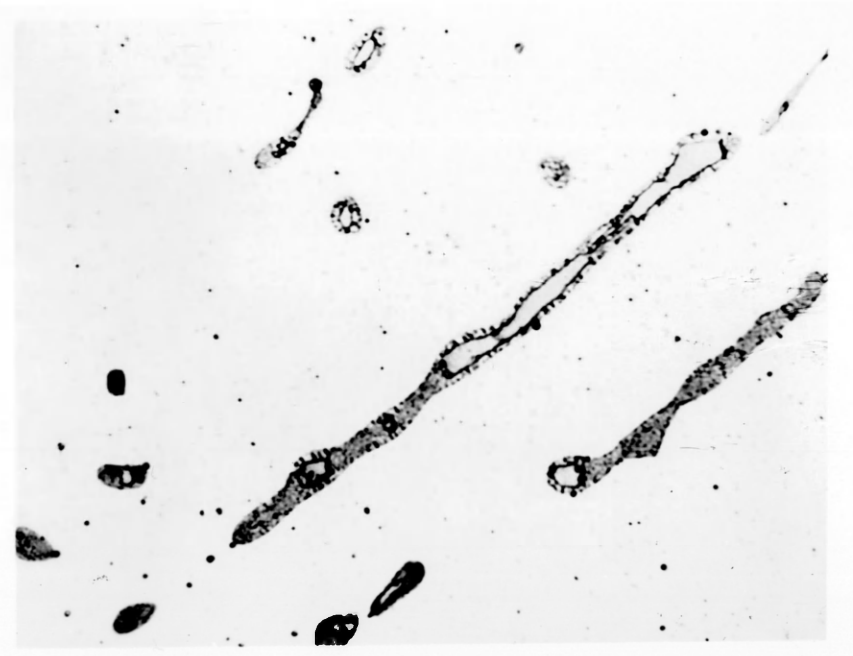


Figure 24 - Solutionized specimen aged at 1350^o F for 1 hr, 1500X, etched electrolytically in Murakami's reagent for 5 sec at 1 v followed by immersion in concentrated Murakami's reagent for 2 min at room temperature. Ferrite in this field is largely consumed.



Figure 25 - Solutionized specimen aged at 1350^o F for 4 hr, 1500X, etched as in figure 24.

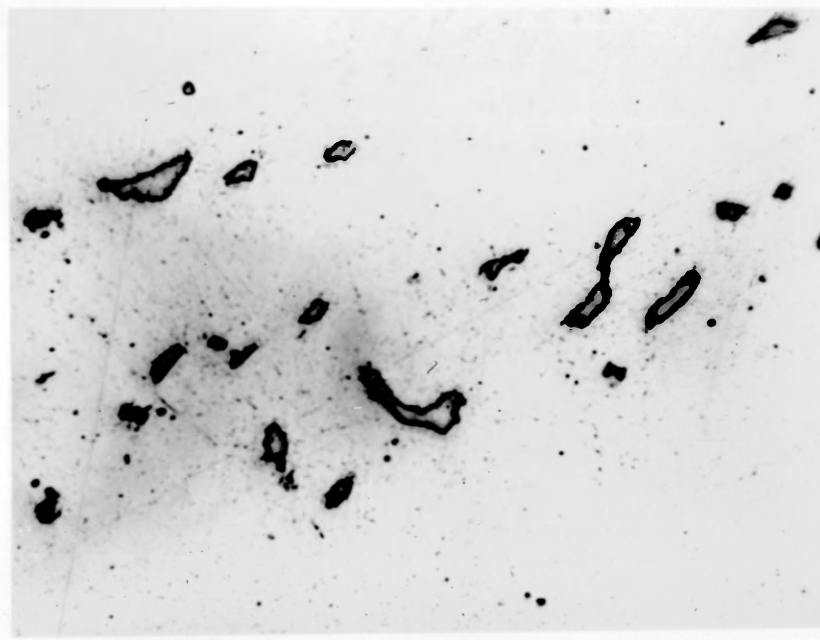


Figure 26 - Solutionized specimen aged at 1350^o F for 4 hr, 1500X, etched in Kalling's reagent for 10 sec followed by light polishing. The unresolved product observed in the preceding photomicrographs is not etched, thus only the untransformed ferrite is shown.

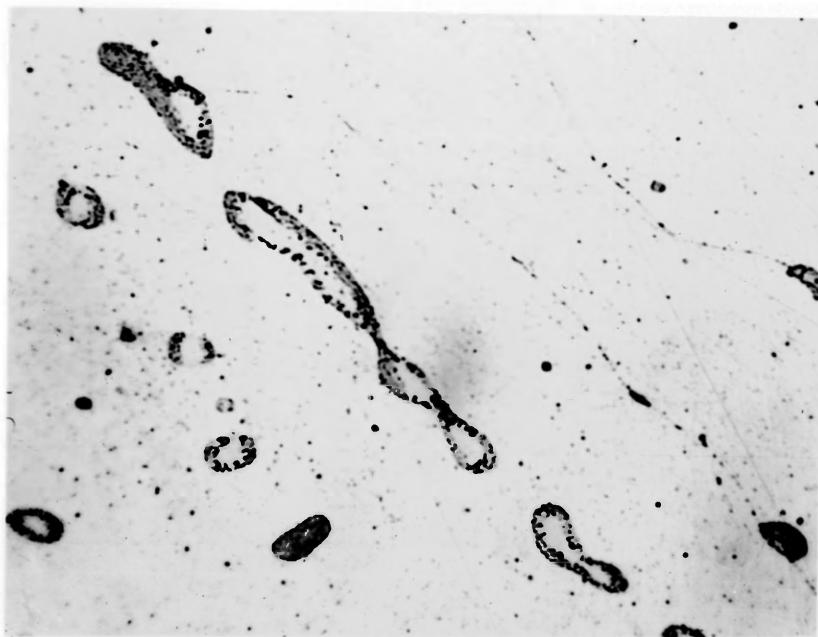


Figure 27 - Solutionized specimen aged at 1350^o F for 24 hr, 1500X, etched in Murakami's reagent for 30 sec at room temperature. Precipitated carbides at the edge of the ferrite areas and at the austenite grain boundaries are revealed.

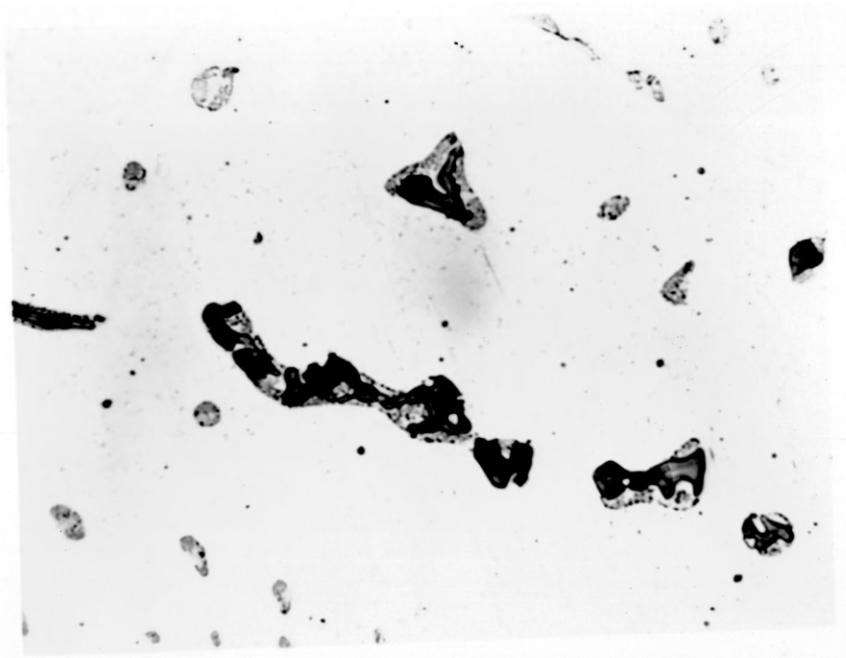


Figure 28 - Solutionized specimen aged at 1350^o F for 24 hr, 1500X, etched in boiling double strength Murakami's reagent for 30 sec. Some of the remaining ferrite as shown in figure 26 has transformed to sigma, shown here as the dark massive phase. Sigma was colored a rich brown when viewed under white light. This is not a typical field. Only approximately 5% of the ferrite transformed to sigma after aging the solutionized specimen for 24 hr.



Figure 29 - Same specimen as figure 28, 1500X, etched electrolytically in chromic acid at 5 v for 5 sec. Sigma and carbides are heavily attacked.

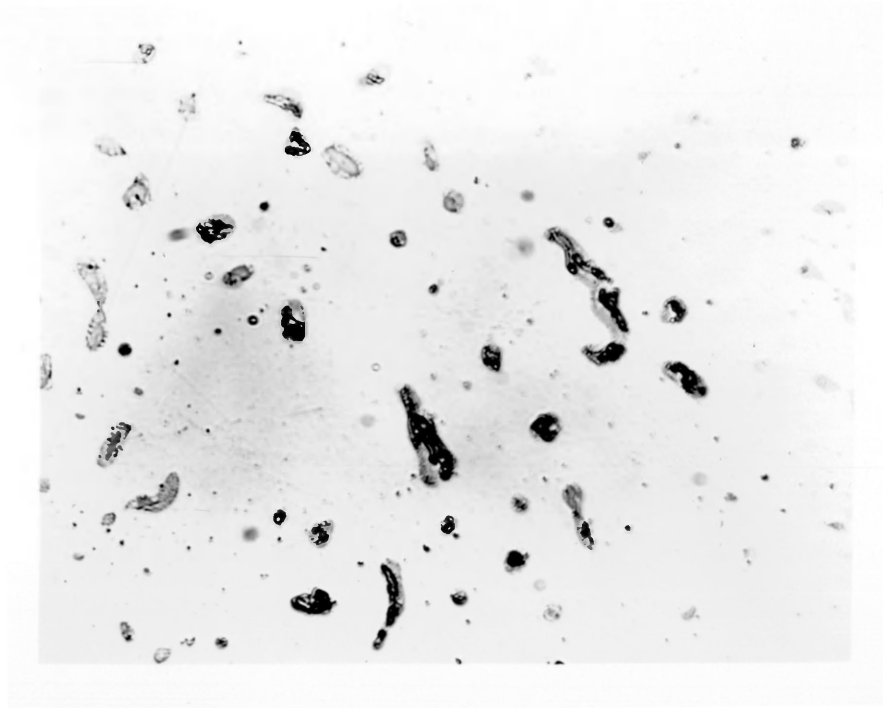


Figure 30 - Solutionized specimen aged at 1350^o F for 24 hr, 1000X, etched in boiling double strength Murakami's reagent for 5 sec. The sigma phase was stained different colors ranging from blue to red to brown in this field.

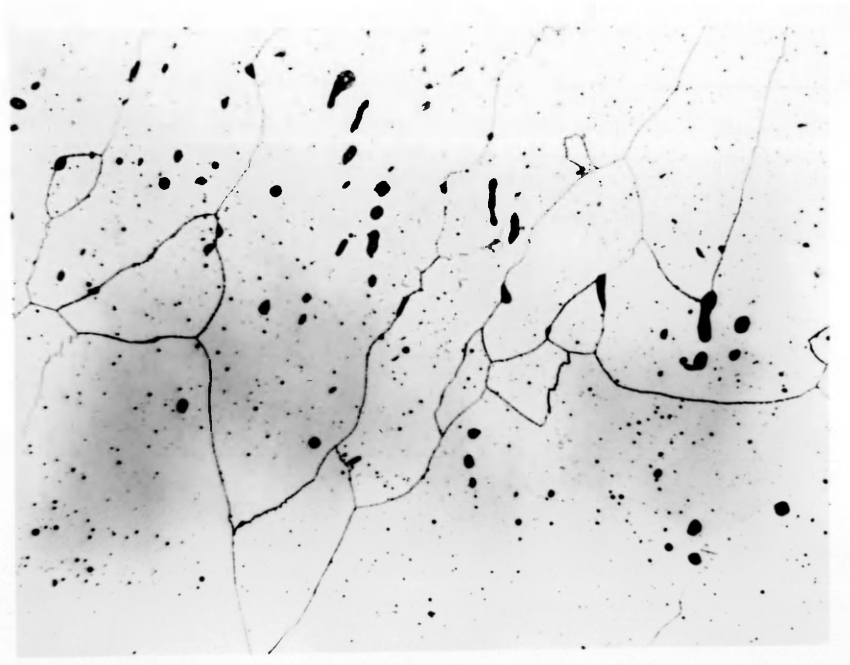


Figure 31 - Solutionized specimen aged at 1350^o F for 24 hr, 500X, etched in FeCl₃-HCl for 15 sec. The epitaxial nature of the growth of dendrites from the unmelted base metal is shown in this photomicrograph of the weld-base metal interface region.

sigma after 500 hr at 1350^o F.

2. Transformation of ferrite to sigma was observed to be much slower in those specimens which were first solutionized. Sigma first appeared at 4 hr aging time and the amount of the total ferrite transformed was still less than 5% after aging for 500 hr.
3. The rate of sigma phase formation appeared to be greatest in a band which roughly followed the weld-base metal interface and was located about 1/3 of the way from the root to the crown of the weld deposit. The first sigma to form in both the as-welded and solutionized structures was found in this region.

X-ray Diffraction

Confirmation of the presence of the phases observed by optical microscopy was provided by x-ray diffraction. It was of particular importance to confirm the presence of the sigma phase because it is often misidentified by optical microscopy, owing to the poor reliability and control of the etchants used in its identification.⁵

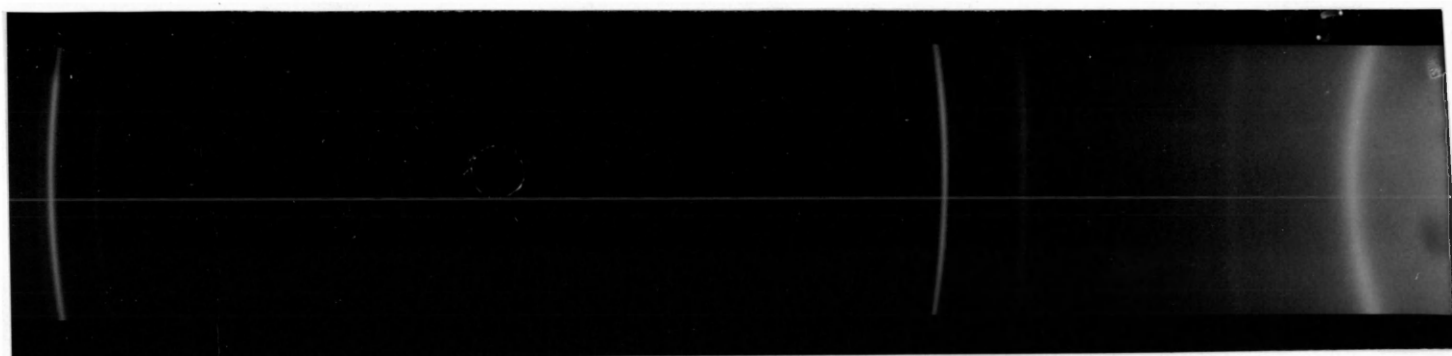
Powder patterns of the weld deposits were obtained using a Debye-Scherrer camera of 10 cm diameter. Unfiltered chromium radiation was used and exposures were generally 4 hr.

First attempts to obtain identifiable powder patterns were made by filing material from the weld deposit and making a specimen rod by applying the filings to a glass fiber

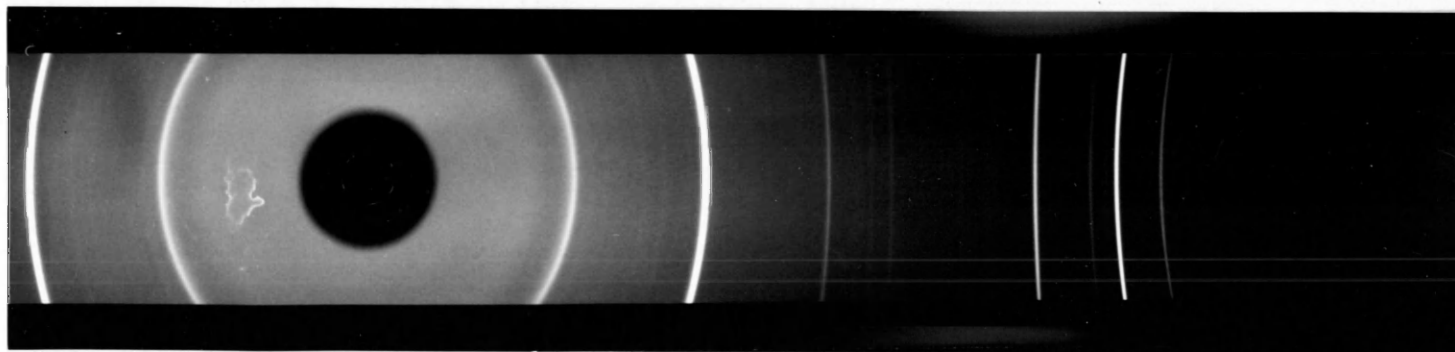
coated with Duco cement. Because of distortion of the crystal lattice by filing, the lines of the patterns so obtained were diffuse and only the lines of austenite and ferrite could be identified. In addition, a significant amount of the austenite was transformed to martensite during the filing as evidenced by a strong attraction of the filings to a magnet. This also contributed to a powder pattern uncharacteristic of the true microstructure. A powder pattern typical of those obtained using filings is shown in figure 32(a).

When the filings were annealed in the air at 1350^o F, a pattern of sharp lines resulted. Unfortunately, this yielded no information about the constituents of the microstructure in its undisturbed state. This is particularly true of the sigma phase which forms at the annealing temperature and is known to be sensitive to prior cold work. A typical powder pattern for the annealed filings is shown in figure 32(b).

The method suggested by Barnett and Troiano³¹ proved successful in obtaining powder patterns of the relatively undisturbed structures. This method consisted of grinding the specimen into a rod of cross-section about 1 mm square. The specimen was then etched electrolytically for 5 min at 6 v in a solution of 45 g FeCl₃ in 100 ml water. This served to dissolve the austenitic matrix, leaving the secondary phases, particularly, sigma, in relief. Figure 33 shows typical patterns obtained by this method. The patterns for



(a)



(b)

Figure 32- Typical x-ray diffraction patterns obtained from cool-worked (a) and annealed (b) filings.

the as-welded specimen (33a) and the specimen which was solution annealed at 2000^o F followed by aging at 1350^o F for 500 hr (33b) show only austenite and ferrite lines. Figure (33c) is the pattern for an as-welded specimen aged for 500 hr at 1350^o F. In addition to the austenite and ferrite lines, at least 8 lines attributable to the sigma phase could be indexed unambiguously. The sigma pattern obtained is identical to that for Fe-Cr sigma in the A.S.T.M. Powder Diffraction File.

Hardness Measurements

Hardness values for representative specimens covering the entire range of heat treatments were obtained using both a Tukon hardness testing instrument and a standard Rockwell hardness tester. A load of 0.1 kg was used with the diamond pyramid indenter on the Tukon tester. Measurements with the Rockwell machine were made on the B scale.

No trends in hardness with heat treatment were observed using either scheme. Measured Rockwell B values were in the range 85-92 and DPH numbers ranged from 195-220. In all cases values were measured in both the base-metal and weld metal areas of the specimen. Again, no difference in hardness was observed between base-metal and weld metal. These results are in accord with those summarized by Lena.¹¹

It was not possible to measure the hardness of the sigma phase alone in these specimens because of the small size of the phase in the microstructure. A typical micro-

hardness traverse in a specimen showing heavy sigma precipitation is shown in figures 34 and 35.

Microprobe Analysis

An attempt was made to follow the redistribution of chromium which results from solidification and heat treatment by electron-probe analysis. The instrument used was a Philips model 4500 electron-probe microanalyzer. The concentration distribution of chromium in the weld metal specimens was displayed on a cathode-ray oscilloscope in a line raster mode synchronous with a line raster scanned by the electron beam on the specimen surface. The analyzer crystal, LiF, was preset to diffract the characteristic CrK radiation, the instantaneous intensity of which was measured by a gas proportional counter. Pulses from the counter with a height within a window preset on a pulse-height selector are recorded in the form of a dot on the oscilloscope. Figure 26 is a Polarid picture of the oscilloscope display showing chromium distribution in the as-deposited weld structure. This picture represents approximately 40 scan cycles during an elapsed time of 10 min. Magnification is approximately 1000X.

Assuming that chromium segregates to some extent into the ferrite areas which solidify between the austenite dendrites, figure 36 should show an image of the same pattern as that shown in figure 9. Although figure 36 shows that chromium distribution is not strictly homogeneous, no de-

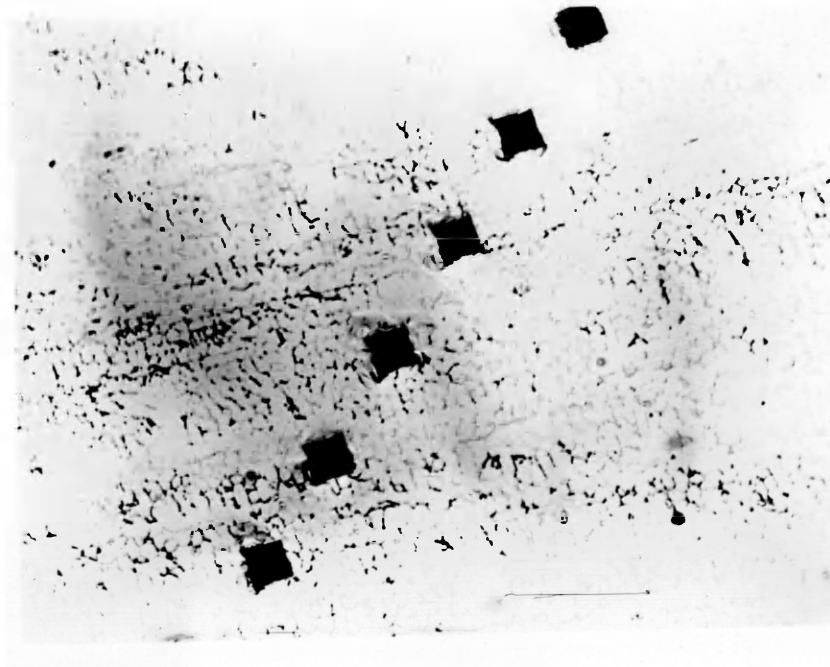


Figure 34 - Microhardness traverse in specimen aged
1350^o F for 1 hr. 0.1 Kg load. 250X.

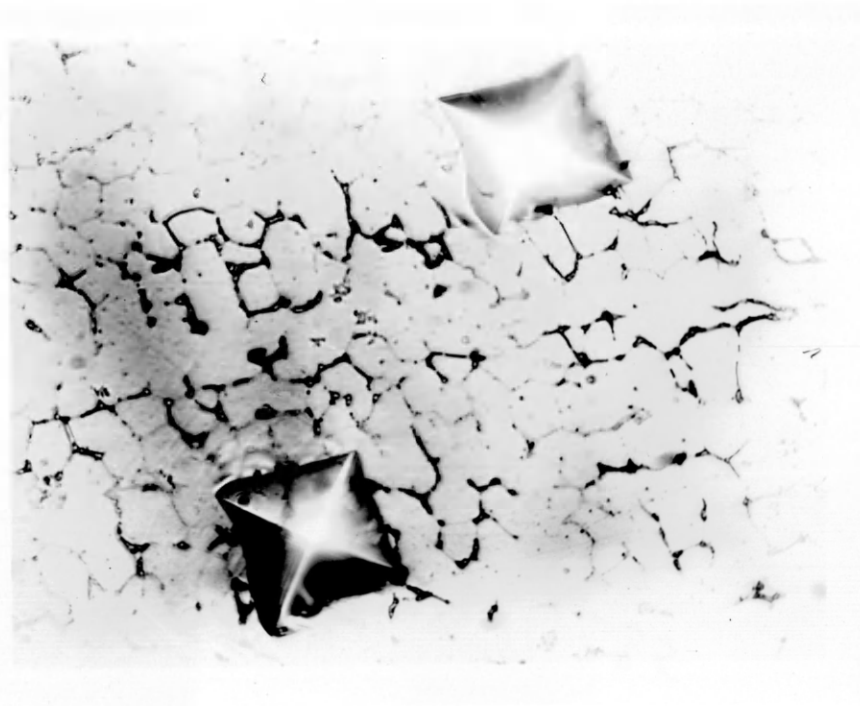


Figure 35 - Microhardness indentations at 1000 X.

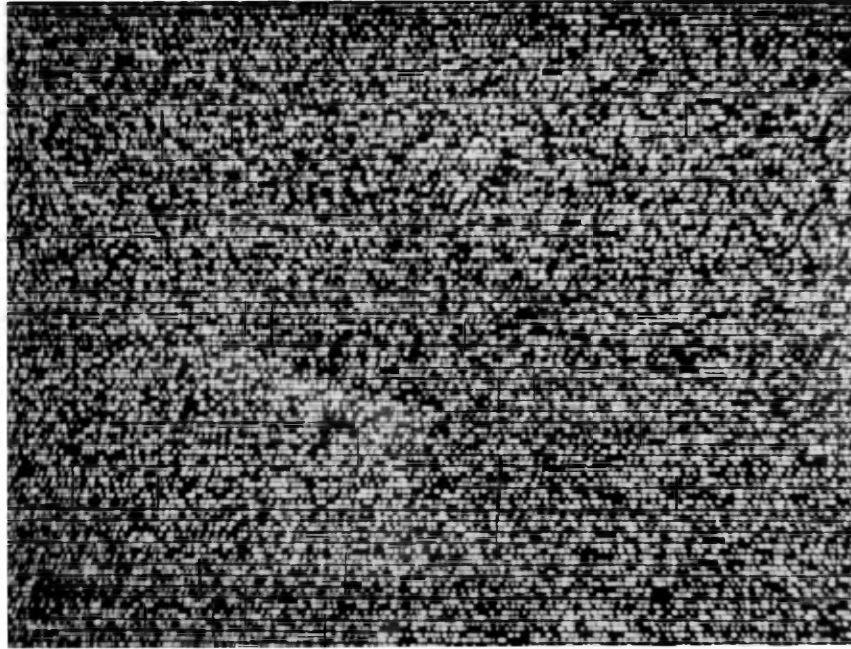


Figure 36 - X-ray image of chromium distribution
in as-deposited weld. 1000X.

finite pattern is immediately evident. A possible reason for the inconclusive results is the fact that typical widths of the ferrite areas as measured from figures 9 and 10 are of the order of 1-3 microns. The size of the well focused electron beam is of this same order of magnitude. Therefore, during a scan the electron beam is only rarely in a fully ferritic area of the microstructure and as a result the information displayed on the oscilloscope represents for the most part either X-rays emitted from the fully austenitic portion of the microstructure, or those emitted from an area partially ferritic and partially austenitic. Daemen and Dept²⁷ found it impractical to observe chromium enrichment in the ferrite phase of a duplex 316 L weld deposit using electron-probe microanalysis. In cast austenitic stainless steel structures containing ferrite pools of the order of 20-30 microns across they were able to show enrichment of chromium in the ferrite phase to approximately 125% of base alloy composition.

It is believed that the distribution of alloying elements in the weld microstructure could be shown in a more successful manner than is shown here by refinement of the measurement technique. By maintaining the electron beam as a fixed point on the specimen surface and using motor-driven specimen translation at a very slow rate while measuring intensity of emitted X-rays by means at a rate-meter recorder, the results would probably be much improved. For this study, however, it was felt that the additional

time required for a detailed analysis using linear traces
was not warranted.

DISCUSSION

Weld Solidification Structure

The microstructure of the as-deposited weld and its subsequent transformations as a result of heat treatment are a direct result of the mode of solidification of the weld. Chalmers³² considers the solidification of a weld to differ from that of any other casting only with respect to the nature of the mold, the initial temperature distribution, and the size of the casting. Given this, the solidification of the weld deposit may be assessed, at least qualitatively, on the basis of solidification theory applicable to any type of solidification process.

Solidification mode. The transformation of a liquid phase to a solid during solidification occurs by a process of nucleation and growth. Reference to figure 18 shows that the solidification of the weld deposit initiates at the base metal and grows epitaxially from the existing structure. Thus the mechanics of growth, and not of nucleation, are of primary importance in discussion of weld solidification.

The photomicrographs of the as-welded structure (figure 9 and 10) show a solidification structure generally termed cellular dendritic. The origin of this structure

may be explained in terms of the mechanics of growth of the crystals from the melt. A stable type of solidification is considered to be that in which a planar interface moves through the liquid. This mode of growth is theoretically characteristic of only the purest of one-component systems in which the heat is extracted from the melt through the solidified crystal. All other systems exhibit some form of unstable growth resulting from the preferential growth of localized areas due to favorable temperature conditions in the melt ahead of the growing crystal. If the volume of liquid metal ahead of a growing crystal is always at a temperature lower than that required for solidification, the growth of the crystal is sustained.

The solidification pattern shown in figure 9 has been described as cellular dendritic. The characteristics of this growth mode have been related in detail by Chalmers.³² This pattern of solidification is typical in weld deposits.³³ Cellular dendrites differ from free dendrites in that the growing crystals interact, forming nearly continuous webs perpendicular to the main direction of growth.

During solidification of a weld we know that heat is supplied from the arc to the melt and extracted through the growing crystals. There must exist then, a means of maintaining a supercooled volume of metal ahead of the growing dendrites which results in the unstable growth structure observed. This supercooling results from the fact the alloy freezes over a range of temperature and is termed con-

stitutional supercooling. In systems which freeze over a range of temperature, the solid which forms from the melt has a different solute content than the liquid from which it forms. The solute (or solvent) which is rejected into the melt at the interface must be distributed in the liquid by diffusion or convection in the liquid. Neither of these processes are instantaneous, thus at any instant the liquid near the interface is of the composition which would be predicted by equilibrium phase relationships at the temperature of the interface. The liquid at a distance from the interface would be of higher or lower solute content than at the interface, depending upon whether the liquidus temperature increases or decrease with solute content. In either case the liquidus temperature of the liquid in contact with the interface is lower than that of the liquid at a greater distance from the interface. The consequence is that supercooling can occur even though the temperature in the liquid is everywhere greater than the liquidus temperature of the bulk liquid.

Segregation. The solidification of the weld deposit appears to have occurred in 3 steps: 1) rapid unstable growth of dendrites, 2) thickening of the dendrite arms at a rate probably much slower than their initial formation, and 3) freezing of the liquid left in the interdendritic regions. Most of solidification theory is based upon studies of 1 or 2 component systems generally solidifying as a single phase. Polyphase solidification has been studied in depth

only in simple binary eutectic systems. At first glance then it seems rather bewildering to attempt to apply the principles of solute redistribution during solidification to a system of at least 6 components as is being studied here. However, by viewing the effect before the cause, the principles may be applied in a qualitative way.

The as-welded microstructure shows that ferrite has solidified in the areas between austenite dendrites. Knowing that the ferrite contains a greater concentration of chromium than does the austenite, we can imagine the system as a simple one in which the solvent is iron and the solute is chromium. Chromium was picked as the solute because of its importance in subsequent transformations of the solid structure.

Because the freezing rate of the weld is very rapid, the solid which forms during the solidification cannot adjust itself to its equilibrium solute concentration at each incremental temperature. Thus the solid which forms displays a cored structure in which the first solid to form is deficient in the solute with respect to the subsequent solid to form and the average solute content of the solid is less than that which would exist under equilibrium conditions. These observations are applicable to the austenite phase in the observed solidification structure. The last liquid to solidify does so as the ferrite phase. Formation of this second single phase suggests a reaction in the system some-

what analogous to the isothermal binary peritectic reaction. Using the reasoning applied to the austenite phase above, this phase could be expected to contain a higher concentration of chromium than would be present under equilibrium conditions. The ferrite phase would also be cored, with the chromium concentrated at the center rather than at the outside of each ferrite area, although this phenomenon would be of a much shorter range than it is in the austenite because of the relative size of the phase areas.

Segregation of the kind described above is generally termed microsegregation or dendritic segregation. Macro or long range segregation is also observed in welds, although to a lesser extent than microsegregation. The nature of dendritic growth tends to minimize long range segregation by trapping the solute which has been rejected at the solid:liquid interface between the dendrite arms. Transverse solute banding may be a significant mode of long range segregation in welds. The banding results from periodic changes in temperature gradient in the liquid. The bands, which occur as surfaces perpendicular to the direction of solidification, are either regions of solute enrichment due to a sudden increase in growth rate or regions of solute depletion due to a sudden decrease in growth rate.³⁴ Although direct observation of this phenomenon was not made in the experimental work presented here, this effect may have manifested itself in the observation of most rapid sigma precipitation along a band of definite location with-

in the structure.

Nature of Observed Transformation

The transformations observed in the as-welded and solutionized weld deposits of the ER 309 filler metal on a type 304 stainless steel base metal will be discussed.

Transformation of the as-welded structure. It has been shown by the photomicrographs of figures 9-21 that the ferrite phase present in the as-welded microstructure transforms to sigma phase when aged at 1350^o F. The extent of this transformation depends upon time at the aging temperature. A small amount of sigma precipitation is observed in the as-welded structure which has been aged for only 20 min. Aging for 24 hr at 1350^o F results in sigma precipitation in approximately 60% of the prior ferrite sites and at 500 hr aging time this figure increases to approximately 80% by visual estimation. An interesting observation with regard to sigma precipitation in the as-welded structure is the fact that ferrite may transform completely to sigma in one interdendritic area while no transformation is observed in an immediately neighboring interdendritic region. This is illustrated in figure 19. Calvo, Bentley, and Baker³³ found that the type of solidification growth structure in a weld deposit, and thus the degree of microsegregation immediately associated with it, is orientation dependent. Thus if we assume that the transformation of sigma is dependent to some degree upon segregation of chromium

during solidification, the observed inhomogeneity in sigma transformation finds probable explanation.

Figure 13 shows the general structure of the as-deposited structure which has been aged for 24 hr. This photomicrograph suggests that sigma is not the only product of the transformation of the ferrite. Actually homogenization of the structure by diffusion would be expected to result in migration of chromium from the ferrite phase to the austenite and transformation of some of the ferrite to austenite. In addition, chromium carbides would be expected to precipitate at the aging temperature. For precipitation of carbides at the austenite:ferrite interface, the depletion in chromium content of the ferrite could cause its transformation of the lower chromium austenite. Holt and Nicholson²⁸ have reported that studies by electron microscopy have shown that the initial breakdown of the ferrite phase results from a finely lamellar mixture of new austenite and sigma growing inward from the ferrite boundary. The etching techniques and optical microscopy used in the present investigation could neither confirm nor deny this observation.

Transformation of the solutionized structure. Heating the as-welded deposit for 1 hr at 2000⁰ F followed by a water quench results in the structure shown in figure 21. The interdendritic ferrite regions have agglomerated into regions bounded by smooth curves, presumably as a result of a driving force provided by a decrease in surface free energy of ferrite:austenite boundary. At the same time the

amount of ferrite in the structure decreased significantly. This is a probable result of redistribution of alloying elements which were segregated as a result of solidification. The ferrite content observed in this specimen is probably very nearly equal to the equilibrium amount for the bulk deposit composition at 2000° F.

Figures 23-27 show the initial breakdown of these agglomerated ferrite areas due to aging at 1350° F. Whether the unresolved product is austenite and carbide or austenite and sigma, the mechanism for transformation is the same. Depletion of the chromium from the ferrite by formation of a phase higher in chromium results in the ferrite being transformed to austenite.

Figures 28-30 show areas of gross transformation of ferrite to sigma phase. It must be remembered that even at an aging time of 500 hr, only about 5% of the ferrite showed transformation to sigma. This results in an amount of sigma in the total structure of less than 1%. Measurement of the amount of sigma in the as-welded structure after aging 24 hr at 1350° F showed almost 18%.

Although the amount of sigma phase present in an alloy of given composition is presumably fixed at any temperature level when equilibrium is attained, no tendency toward this situation is evident after 500 hr at 1350° F. For practical purposes this type of equilibrium may never be obtained. Thus, prior treatment is an important factor in the transformations observed. The beneficial effect of prior heat

treatment in the 1925-2000^o F range in reducing the embrittlement of duplex weld metals has been recognized by Malone.³⁵ The effect is attributed to the agglomeration of the ferrite pools and reduction of the amount of ferrite in the structure. Sigma formed later is then reduced in amount and present in a discontinuous pattern. This, however, is only a description of the observed result. Evidence from the present study indicates that significant sigma phase formation is primarily a result of segregation of sigma forming elements during weld solidification. Annealing of the deposit at 2000^o F eliminates this segregation by homogenization and greatly reduces the tendency toward sigma formation.

CONCLUSIONS

From the literature survey and results of the experimental work, the following conclusions can be drawn:

1. Ferrite transforms readily to sigma phase in the as-welded deposit aged at 1350⁰ F.
2. Rapid transformation of ferrite to sigma in the weld deposit aged at 1350⁰ F is attributable to segregation of sigma forming elements in the ferrite phase during weld solidification.
3. Heating of the weld deposit for 1 hr at 2000⁰ F followed by water quenching causes a significant decrease in the amount of ferrite in the deposit. This is a result of homogenization of the solidification structure.
4. A marked reduction in the rate and amount of sigma phase formation results from prior heat treatment at 2000⁰ F. Again, this results from alloy homogenization.

SUGGESTIONS FOR FURTHER RESEARCH

Some of the factors involved in the kinetics of sigma phase formation were examined in this investigation. Results indicate that alloy composition, both bulk and local, probably exerts the greatest influence on the formation of this phase. Although it may be necessary to undertake similar studies with regard to specific processes and materials in which sigma phase may be a problem, it is felt that additional studies of sigma kinetics is unwarranted.

The area of weld solidification would seem to be an exceptionally fruitful subject for further research. This field has not been investigated extensively and quantitative treatments are virtually non-existent. The present study suggests several specific areas of possible importance:

- 1.) Welding process parameters are currently established on an empirical basis. Evaluation of a process is based upon the performance of a welded joint against a specified standard in tests of mechanical properties. Correlation of mechanical properties with weld solidification structure, and in turn correlation of solidification structure with welding parameters, should lead to a sound

basis for selecting optimum welding parameters for any joining situation.

2.) Epitaxial growth of crystals in the weld deposit from those in the unmelted base material is generally observed in welds. Investigation of the influence of preferentially oriented base metal grains on the weld solidification structure could be useful in predicting resulting mechanical properties.

3.) Long and short range segregation in weld deposits can have a marked effect on the corrosion resistance of welds. An investigation directed toward minimizing segregation by adjustment of welding parameters would be of practical significance.

LITERATURE CITED

1. Am. Soc. for Metals, 1948, Metals handbook: Metals Park, Ohio, A.S.M., p. 1194-1195, 1211, 1260-1261.
2. Lagneborg, R., 1964, The martensite transformation in 18% Cr-8% Ni steels: Acta Metallurgia, v. 12, no. 7, p. 823-843.
3. Clause, F. J., 1969, Engineer's guide to high-temperature materials: Menlo Park, Cal., Addison-Wesley Pub. Co., p. 92.
4. Schaeffler, A.L., 1949, Constitution diagram for stainless steel weld metal: Metal Progress, v. 56, no. 5, p. 680.
5. Thielsch, Helmut, 1950, Physical metallurgy of austenitic stainless steels: Welding Jour., v. 29, no. 12, p. 577s-621s.
6. Hull, F.C., 1967, Effect of delta ferrite on the hot cracking of stainless steel: Welding Jour., v. 46, no. 9, p. 399s-409s.
7. Brick, R.M., Gordon, R.B., and Phillips, Arthur, 1965, Structure and properties of alloys: New York, McGraw-Hill Book Co., p. 342.
8. Pinnow, K.E., and Moskowitz, A., 1970, Corrosion resistance of stainless steel weldments: Welding Jour., v. 49, no. 6, p. 278s-284s.
9. Bain, E.C. and Griffiths, W.E., 1927, An introduction to the iron-chromium-nickel alloys: Trans. A.I.M.E. Met. Soc., v. 75, p. 166.
10. A.S.T.M. Symposium on the nature, occurrence, and effects of sigma phase, 1950, A.S.T.M. Spec. Tech. Pub. 110.
11. Lena, A.J., 1954, Sigma phase - a review: Metal Progress, v. 66, no. 1, p. 86, no. 2 p. 94, no. 3 p. 122.
12. Hall, E.O. and Algie, S.H., 1966, The sigma phase: Journal of the Institute of Metals, Met. Rev., v. 11, P. 61-88.

13. Cook, A.J. and Jones, F.W., 1943, The brittle constituent of the iron-chromium system (sigma phase): Jour. Iron and Steel Inst., v. 148, p. 217-226.
14. Shortsleeve, E.J. and Nicholson, M.E., 1951, Transformations in ferritic chromium steels between 1100^o and 1500^o F: Trans. A.S.M., v. 43, p. 142-160.
15. Hattersley, B. and Hume-Rothery, W., 1966, Constitution of certain austenitic steels: Jour. Iron and Steel Inst., v. 204, p. 683-701.
16. Nicholson, M.E., Samans, C.H., and Shortsleeve, E.J., 1952, Composition limits of sigma formation in nickel-chromium steels at 1200^o F: Trans. A.S.M., v. 44, p. 601.
17. Tisinai, G.F., Stanley, J.K., and Samans, C.H., 1956, Sigma nucleation in stainless steels: Jour. of Metals, A.I.M.E., v. 8, no. 5, p. 600-604.
18. Simpkinson, T.V., 1957, Metallography of titanium-stabilized 18-8 stainless steel: Trans. A.S.M., v. 49, p. 721-746.
19. Gillman, J.J., Koh, P.K., and Zmeskal, O., 1949, Delta ferrite formation and its influence on the formation of sigma in a wrought heat-resisting steel: Trans. A.S.M., v. 41, p. 1373-1399.
20. Singhal, L.K., and Martin, J.W., 1968, The formation of ferrite and sigma phase in some austenitic stainless steels: Acta Met., v. 16, p. 1441-1451.
21. Albritton, O.W. and Kadlecek, P.E., 1968, Microstructural variations in welded austenitic stainless steel caused by heating at 1350^o F: Welding Jour., v. 47, no. 2, p. 73s-81s.
22. Singhal, L.K. and Vaidys, M.L., 1969, Precipitation of sigma phase in a duplex Fe-Cr-Ni-Ti Alloy: Trans. A.S.M., v. 62, p. 879-885.
23. Streicher, M.A., 1964, Effect of heat treatment, composition, and microstructure on corrosion of 18 Cr-8 Ni-Ti stainless steels in acids: Corrosion, v. 20, p. 57t-72t.
24. Duhaj, P., Ivan, J., and Makovicky, E., 1968, Sigma phase precipitation in austenitic steels: Jour. Iron and Steel Inst., v. 206, p. 1245-1251.